Elsevier Editorial System(tm) for Science of the Total Environment
Manuscript Draft

Manuscript Number:

Title: Vacuum ultraviolet photolysis of diclofenac and the effect of the treated aqueous solutions on the proliferation and migratory responses of Tetrahymena pyriformis

Article Type: Full Length Article

Keywords: advanced oxidation process; chemotaxis; hydroxyl radical; non-steroidal anti-inflammatory drug; photodegradation; toxicity

Corresponding Author: Dr. Krisztina Gajda-Schrantz, assistant professor

Corresponding Author's Institution: Research Group of Environmental Chemistry, University of Szeged AND Department of Inorganic and Analytical Chemistry, University of Szeged AND EMPA, Swiss Federal Laboratories for Material Testing and Research, Laboratory for High Performance Ceramics

First Author: Eszter Arany

Order of Authors: Eszter Arany; Júlia Láng; Dávid Somogyvári; Orsolya Láng; Tünde Alapi, professor's assistant; István Ilisz; Krisztina Gajda-Schrantz, assistant professor; András Dombi, professor; László Kőhidai; Klára Hernádi, professor

Abstract: The effect of dissolved O2, phosphate buffer and the initial concentration of diclofenac were studied on the vacuum ultraviolet photolysis of this contaminant molecule. The kinetic measurements were completed with the characterization of the irradiated, multicomponent samples with the proliferation and migratory responses (in sublethal concentrations) of the bioindicator eukaryotic ciliate Tetrahymena pyriformis. The results suggest that not only hydroxyl radicals but also hydrogen atoms and hydroperoxyl radicals might contribute to the degradation of diclofenac. Among the aromatic by-products of diclofenac a hydroxilated derivative, 1-(8-chlorocarbazolyl)acetic acid and 1-(8-hydroxycarbazolyl)acetic acid) could be detected. Biological activity of photoexposed samples reflected chemical transformation of diclofenac and was also dependent on the used level of dissolved O2. The increase in toxicity of samples taken at different irradiation times did not exceed a factor of two. Our results suggest that the combination of vacuum ultraviolet photolysis with toxicity and chemotactic measurements can be a valuable method for the investigation of the elimination of micropollutants.

Suggested Reviewers: Thomas Oppenländer
professor, Faculty of Mechanical and Process Engineering, Hochschule Furtwangen University
op@hs-furtwangen.de
Prof. Thomas Oppenländer is an expert in the field of advanced oxidation technologies and vacuum ultraviolet photolysis, which is the degradation method used in our study.

Petr Solich
professor
Petr.Solich@faf.cuni.cz

Roberto Andreozzi
professor, Dipartimento di Ingegneria Chimica, Università di Napoli Federico II

roberto.andreozzi@unina.it
Prof. Roberto Andreozzi is an expert in toxicological researches.

Kristof Demeestere
professor, Research Group EnVOC, Department of Sustainable Organic Chemistry and Technology, Ghent University
Kristof.Demeestere@UGent.be
Prof. Kristof Deemestre is an expert in the field of advanced oxidation processes.

Opposed Reviewers:

Dear Editor,

during a bilateral relationship between the Semmelweis University and the University of Szeged the novel combination of an advanced oxidation process (the vacuum ultraviolet photolysis) and the characterization of the toxic and chemotactic properties of the treated multicomponent solutions was performed. As target molecule the non-steroidal anti-inflammatory drug diclofenac and as bioindicator the eukaryotic ciliate *Tetrahymena pyriformis* was choosen. In this study the effect of dissolved O_2, phosphate buffer and the initial concentration of diclofenac were studied on the vacuum ultraviolet photolysis of this contaminant molecule. Suggestions were given for the chemical structure of formed aromatic by-products. The effect of dissolved O_2 on the proliferation and migratory behavior of the ciliate was also investigated. Our results suggest that the combination of vacuum ultraviolet photolysis with toxicity and chemotactic measurements can be a valuable method for the investigation of the elimination of micropollutants.
We hope you will consider our work worth publishing and I am looking forward to hearing from you soon.

Yours faithfully,
Krisztina Gajda-Schrantz

Graphical Abstract (for review)

$$H_2O + h\nu_{172\ nm} \rightarrow H^{\bullet} + {}^{\bullet}OH \xrightarrow{+\ DICL} products$$

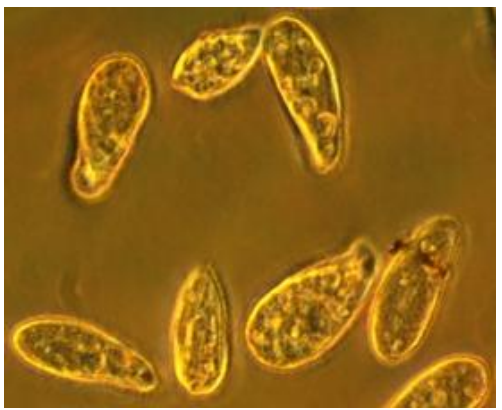

Tetrahymena pyriformis

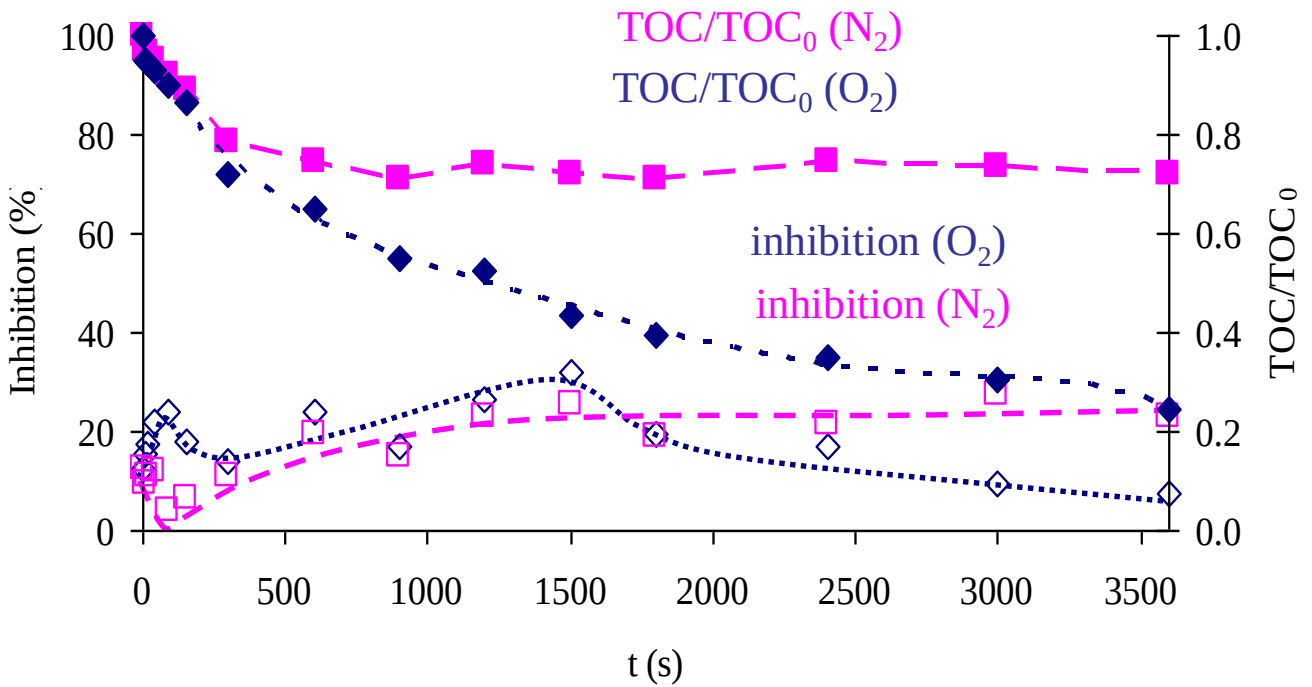

Highlights

- $H^{\bullet}$ and $HO_2^{\bullet}$ react with diclofenac with similar reaction rate.
- The radical scavenging effect of phosphates seems to be negligible.
- $HO_2^{\bullet}$ contributes only in higher concentrations to the degradation of diclofenac.
- Toxicity of VUV treated samples vary with irradiation time and operating condition.
- Treated samples retain chemorepellent character of the parent compound.

Vacuum ultraviolet photolysis of diclofenac and the effect of the treated aqueous solutions on the proliferation and migratory responses of *Tetrahymena pyriformis*

Eszter Arany[1], Júlia Láng[2], Dávid Somogyvári[1], Orsolya Láng[2], Tünde Alapi[1,3], István Ilisz[3], Krisztina Gajda-Schrantz[1,3,4,*], András Dombi[1], László Kőhidai[2], Klára Hernádi[1]

[1]Research Group of Environmental Chemistry, Institute of Chemistry, University of Szeged, 6720 Szeged, Rerrich Béla tér 1, Hungary

[2]Department of Genetics, Cell- and Immunobiology, Semmelweis University, 1089 Budapest, Nagyvárad tér 4, Hungary

[3]Department of Inorganic and Analytical Chemistry, University of Szeged, 6720 Szeged, Dóm tér 7, Hungary

Abbreviations

AOP: advanced oxidation process
c-AMP: cyclic adenozine monophosphate
c-GMP: cyclic guanozine monophosphate
Chtx. Ind.: Chemotaxis Index
DICL: diclofenac
k: reaction rate constant
k': apparent reaction rate constant
k_{DICL}: second order reaction rate constant between DICL and $^{\bullet}OH$
$k_{HPO_4^{2-}}$: second order reaction rate constant between HPO_4^{2-} and $^{\bullet}OH$
$k_{H_2PO_4^-}$: second order reaction rate constant between $H_2PO_4^-$ and $^{\bullet}OH$
$[^{\bullet}OH]_{SS}$: the steady state concentration of hydroxyl radicals
PB: phosphate buffer
PhAC: pharmaceutically active compound
PIP3: phosphatidylinositol (3,4,5)-triphosphate
$R^{\bullet}$: carbon centered radical
r_{DICL}: reaction rate between DICL and $^{\bullet}OH$
$r_{HPO_4^{2-}}$: reaction rate between HPO_4^{2-} and $^{\bullet}OH$
$r_{H_2PO_4^-}$: reaction rate between $H_2PO_4^-$ and $^{\bullet}OH$
$ROO^{\bullet}$: peroxyl radical
SE: standard errors of the mean
WWTP: wastewater treatment plant

[4]EMPA, Swiss Federal Laboratories for Material Testing and Research, Laboratory for High Performance Ceramics, 8600 Dübendorf, Überlandstrasse 129, Switzerland

[*]Corresponding author: Phone: +36-62-544338; email: sranc@chem.u-szeged.hu

Abstract

The effect of dissolved O_2, phosphate buffer and the initial concentration of diclofenac were studied on the vacuum ultraviolet photolysis of this contaminant molecule. The kinetic measurements were completed with the characterization of the irradiated, multicomponent samples with the proliferation and migratory responses (in sublethal concentrations) of the bioindicator eukaryotic ciliate *Tetrahymena pyriformis*. The results suggest that not only hydroxyl radicals but also hydrogen atoms and hydroperoxyl radicals might contribute to the degradation of diclofenac. Among the aromatic by-products of diclofenac a hydroxilated derivative, 1-(8-chlorocarbazolyl)acetic acid and 1-(8-hydroxycarbazolyl)acetic acid) could be detected. Biological activity of photoexposed samples reflected chemical transformation of diclofenac and was also dependent on the used level of dissolved O_2. The increase in toxicity of samples taken at different irradiation times did not exceed a factor of two. Our results suggest that the combination of vacuum ultraviolet photolysis with toxicity and chemotactic measurements can be a valuable method for the investigation of the elimination of micropollutants.

Keywords: advanced oxidation process, chemotaxis, hydroxyl radical, non-steroidal anti-inflammatory drug, photodegradation, toxicity

1 Introduction

Diclofenac (DICL, 2-(2-(2,6-dichlorophenylamino)phenyl)acetic acid) is an arylacetic acid non-steroidal anti-inflammatory drug used for multiple indications in both human and veterinary medicine. Consequently it is massively consumed worldwide representing 960 tons estimated global annual consumption (Zhang et al., 2008). It was one of the pharmaceutically active compounds (PhACs) first described to affect the wellbeing of living organisms when it was directly linked to the massive population decline in the 1990s of the different vulture species of the Indian subcontinent (Oaks et al., 2004).

Moreover, together with carbamazepine, it is the most frequently detected PhAC in water bodies (Zhang et al., 2008). The main route of entry into the aquatic environment is via the sewage where – following human administration of the drug – it is excreted unchanged (2 – 15 %) and in form of hydrolysable conjugates (1 – 15 %) (Khan and Ongerth, 2004; Ternes, 1998). Furthermore, as both the biodegradation and sorption of DICL were found to be minimal (Buser et al., 1998; Zwiener and Frimmel, 2003) at wastewater treatment plants (WWTPs) its removal is pretty low – usually between 20 – 40 % – resulting in the accumulation of DICL in surface waters. Depending on the geographical location and the type of water the environmental concentrations range from the low ng L^{-1} to 1000 ng L^{-1}. Environmental loads were recently reported by Pal et al., 2010; Ratola et al., 2012; Santos et al., 2010; for surface- and wastewaters, by Lapworth et al., 2012 for ground waters and by Daughton, 2010; Vulliet et al., 2011 for drinking waters.

Concerning its biological effects on ecosystems a large number of studies were carried out using diverse species including bacteria, algae, ciliates, crustacean or fish (Santos et al., 2010). Even though based on these studies the acute ecotoxicity of DICL is unlikely, there is still a lack of knowledge about its chronic effect, its synergistic toxicity with other drugs and most importantly about the toxicity of its metabolites and degradation products (Zhang et al., 2008).

The above mentioned data about the wide range loading of environment with DICL explain that the improvement of water purifying techniques is needed, which could be accomplished by using advanced oxidation processes (AOPs) (Kruithof et al., 2007; Legrini et al., 1993). The most significant among them are radiolysis, photochemical

processes, ozone based methods, homogeneous or heterogeneous photocatalytic techniques.

Both ultraviolet (UV) lamps and the UV range of solar irradiation was found to efficiently transform DICL with quantum yield values in the range of 0.03 – 0.32 (Boreen et al., 2003; Buser et al., 1998; Moore et al., 1990; Poiger et al., 2001). However, UV doses typically used during water disinfection in water treatment plants (400 J m^{-2}) are sufficient to eliminate only ~ 30 % of DICL (Canonica et al., 2008; Meunier et al., 2006).

AOPs are based on the generation of reactive radicals, which induce the degradation of pollutant molecules. Among the formed radicals hydroxyl radical ($^{\bullet}OH$) is the most reactive and less selective one, reacting with a rate constant of $10^7 – 10^{10}$ mol^{-1} L s^{-1} with organic and inorganic compounds (Anbar and Neta, 1967). The reaction between $^{\bullet}OH$ and DICL follows second order kinetics, the reaction rate constant (k_{DICL}) being between $(0.6 – 2.4) \times 10^{10}$ mol^{-1} L s^{-1} (Aruoma and Halliwell, 1988; Huber et al., 2003; Parij et al., 1995; Yu et al., 2013). Using the steady state approximation for the concentration of $^{\bullet}OH$ ($[^{\bullet}OH]_{SS}$), which therefore might be incorporated in the apparent reaction rate constant ($k' = k \times [^{\bullet}OH]_{SS}$) in homogeneous systems, the kinetics is usually treated as a pseudo first-order reaction.

The significance of reactive radicals is supported by the efficiency of ozonation, homogeneous and heterogeneous photocatalyses (Bernabeu et al., 2011; Huber et al., 2003; Klamerth et al., 2009; Perez-Estrada et al., 2005; Sein et al., 2008; Vogna et al., 2004)

For the determination of the effect of $^{\bullet}OH$ during DICL degradation, $^{\bullet}OH$ should be formed during the primary step of the used method. Suitable techniques are therefore radiolysis and VUV photolysis (1).

$$H_2O + h\nu_{172\ nm} \rightleftharpoons (H_2O)^* \rightarrow H^{\bullet} + {}^{\bullet}OH \quad (1)$$

As it can be seen from (1) hydrogen atoms ($H^{\bullet}$) and $^{\bullet}OH$ are the primary radicals, although in case of radiolysis hydrated electrons (e_{aq}^-) and $^{\bullet}OH$ form. Radiolytic experiments revealed that both $^{\bullet}OH$ and e_{aq}^- are effective in the degradation of DICL, the latter species having a lower contribution to the mineralization (Homlok et al., 2011; Yu et al., 2013). However, to our best knowledge VUV photolysis of DICL has not yet been investigated.

The use of AOPs as a post treatment could enhance the efficiency of DICL elimination in WWTPs and in this way could decrease the ecotoxicological risk of this compound in the environment. Although in some cases the increase of the toxic effect was observed (*e.g.* in case of photolytic or photocatalytic treatments) because of the formation of compounds more harmful than DICL itself (Calza et al., 2006; Schmitt-Jansen et al., 2007), prolonged treatments resulted in the detoxification of the solutions (Calza et al., 2006; Homlok et al., 2011; Yu et al., 2013).

In the present study our aims were i) to describe the VUV photolysis of DICL; ii) to study the influence of the operating conditions on the kinetics and efficiency of DICL degradation; iii) to characterize the effects of the samples taken at different times of the photolytic degradation on the proliferation and – in sublethal concentrations – on the migratory responses of the bioindicator eukaryotic ciliate *Tetrahymena pyriformis*. The presented combination of the VUV photolysis and the investigation of the biological

effect of the treated multicomponent solutions would be beneficial also in case of other PhACs.

2 Material and methods

2.1 Chemicals and reagents

All the chemicals were of analytical purity and were used without further purification. From the sodium salt of DICL (Sigma, St. Louis, MO, USA) 1.0×10^{-5} mol L^{-1}, 4.0×10^{-5} mol L^{-1}, 7.0×10^{-5} mol L^{-1} and 1.0×10^{-4} mol L^{-1} solutions were prepared in ultrapure Milli-Q water (MILLIPORE Milli-Q Direct 8/16, Billerica, MA, USA) or in phosphate buffered solution (PB) in case of toxicity and chemotaxis experiments. PB of pH = 7.4 contained 1.1×10^{-3} mol L^{-1} NaH_2PO_4 (≥ 99%, Spektrum 3D, Debrecen, Hungary) and 1.9×10^{-3} mol L^{-1} Na_2HPO_4 (≥ 99.0%, Fluka, Buchs, Germany) in Milli-Q water.

2.2 The photochemical apparatus

For the VUV measurements (Fig. 1) a xenon excimer lamp (3; Radium Xeradex™, length 130 mm, external diameter 40 mm, 20 W electric input power) emitting at 172±14 nm was placed in the center of a water cooled, triple-walled tubular reactor (4; length 220 mm, external diameter 50 mm, the inner wall being made of Suprasil® quartz). The photon flux of the light source was determined with methanol actinometry (Oppenlander and Schwarzwalder, 2002) and was found to be 3×10^{-6} mol_{photon} s^{-1}. The treated solution (250 mL) was circulated with 375 mL min^{-1} within the two inner walls of the reactor (4) in a 2 mm thick layer and the reservoir (6) using a Heidolph Pumpdrive 5001 peristaltic

pump (5). Water was circulated between the outer walls of both the reactor (4) and the reservoir (6) to regulate the temperature to 25±0.5 °C. Nitrogen (> 99.99% purity, Messer, Budapest, Hungary) or oxygen (> 99.99% purity, Messer, Budapest, Hungary) was bubbled (600 mL min^{-1}) through the solution in the reservoir to attain deoxygenated or O_2 saturated conditions, respectively. The injection of N_2 and O_2 was started 30 or 15 min before each experiment, respectively and was continued till the end of the irradiation. The pH of the irradiated solutions was measured with an inoLab pH 730p instrument introducing the measuring electrode directly into the reservoir (6).

All the presented results are the average of two-five experiments, the error bars showing the standard deviation of the measured values.

2.3 High performance liquid chromatography with mass spectrometry

Samples were analysed on an Agilent 1100 type instrument with UV-DAD and MS detection using a C18 (Phenomenex Kinetex C_{18}, 100 × 4.6 mm, 2.6 μm) column. As eluent 1% aqueous acetic acid (HPLC grade, VWR, Fontenay-sous-Bois, France) solution and acetonitrile (ultra gradient HPLC grade, J.T.Baker, Deventer, the Netherlands) was used in 1:1 ratio, with a 0.8 mL min^{-1} flow rate. The quantification wavelengths for the UV detector were 240, 273 and 280 nm. For the MS detection electrospray ionization was used in the negative ion mode. Nitrogen as drying gas (300 °C, 12 L min^{-1}), fragmentor voltage of 70 V (in case of measuring by-products A and B) or 80 V (in case of measuring by-product C), nebulizer pressure of 3.4 bar and capillary voltage of 1000 V were used.

The separation of the aliphatic by-products was carried out on a GROM-RESIN ZH (Herrenberg-Kayh, 250 × 8 mm, 8 μm) column, with detection at 206 nm. As eluent 0.01 mol L^{-1} sulfuric acid (AnalR NORMAPUR, VWR, Fontenay-sous-Bois, France) was used in this case with a 0.8 mL min^{-1} flow rate.

2.4 Adsorbable organic halogen content measurements

For the determination of the adsorbable organic halogen (AOX) content of the solutions 30 mL sample was pressed with 3 mL min^{-1} flow rate through two quartz tubes containing 2 × 50 mg active carbon in the APU2 sample preparation module (Analytik Jena AG, Jena, Germany). Inorganic halogens were washed from the surface of the carbon with a solution containing 0.2 mol L^{-1} $NaNO_3$ (VWR, Leuven, Belgium) and 0.14 mol L^{-1} HNO_3 (Farmitalia Carlo Elba S.p.A., Milano, Italy). The carbon containing columns were then burned in O_2 (> 99.99% purity, Messer, Budapest, Hungary) stream at 950 °C and their halogen content was measured using a microcoulometric method in a multi X 2500 instrument (Analytik Jena AG, Jena, Germany).

2.5 Total organic carbon content measurements

For the determination of the total organic carbon (TOC) content of the solutions a multi N/C 3100 instrument (Analytik Jena AG, Jena, Germany) was used. At first, 2 mL 10 v/v % H_3PO_4 (purchased from SAFC, St. Louis, MO, USA) was added to 500 μL solution to release the total inorganic carbon (TIC) of the sample in form of CO_2. The second 500 μL of the sample was then burned in O_2 (> 99.995% purity, Messer, Budapest, Hungary) stream at 800 °C. The formed CO_2 referred to the total carbon (TC) content of the

sample. The amount of CO_2 was measured with a non-dispersive infrared absorption detector in both cases. The TOC content of the solutions was determined from the difference of the TC and TIC values.

2.6 Kinetic modelling

The formal *k'* values of DICL degradation were determined by performing a nonlinear model fit on the concentration values measured during HPLC analyses, with the help of Mathematica 8 (Wolfram) software. It has to be mentioned that our system is very inhomogeneous. On the one hand, the VUV photons are absorbed in a very thin water layer (< 0.1 mm) and therefore only a thin-walled hollow cylindrical volume is irradiated from the solution, near the quartz/water interface. On the other hand, the experimental setup consisted of a partly-irradiated reactor and a reservoir. Thus, the determined (virtual) *k'* values refer to the total transformation rate of DICL under the used experimental conditions.

2.7 Cell culturing

The eukaryote ciliate *Tetrahymena pyriformis* GL was maintained in 0.1% yeast extract and 1% Bactotriptone (Difco, Michigan, USA) containing culture media at 28°C. In all experiments 24 h exponential growth phase cultures were used.

2.8 Proliferation inhibition assay

For toxicity assay samples from the photolysis (0 s, 10 s, 20 s, 40 s, 1.5 min, 2.5 min, 5 min, 7.5 min, 10 min, 15 min, 20 min, 25 min, 30 min, 35 min, 40 min, 50 min and 60

min) of 1.0×10^{-4} mol L^{-1} DICL in PB were taken. Proliferation inhibition assay was carried out as described by Láng J. and Kőhidai L., 2012 with initial cell number of 10^3 cells in the core blocks of 60 wells in 96 well microtiter plates (Sarstedt AG, Nümbrecht, Germany) incubated at 28°C for 24 h. Samples were diluted to 1 %, 5 % and 25 % (v/v) in cell culture media. The highest concentration was determined in preliminary experiments in order to avoid massive disintegration of the cells due to osmotic shock that would disturb the objective evaluation of the toxic effect of the samples. In these experiments cells were incubated with serial dilution of DICL free PB for 24 h, then their number and morphology was evaluated under microscope (Zeiss Axio Observer, Göttingen, Germany). At the end of the proliferation inhibition assay cell number was determined using the impedimetric CASY TT cell counter (Innovatis-Roche, Rotkreuz, Switzerland). Cells were counted using 150 μm diameter capillary and counted events in the 10 – 100 μm diameter range were considered as cells. Potential aggregation of cells was corrected during the cell number evaluation by the aggregation factor determined as the ratio of the peak cell diameter and average cell diameter. Inhibitory effect of VUV treated samples was determined by normalizing the number of cells in treated sample wells to the cell number in negative control wells. These wells contained culturing media with the appropriate volume proportion of PB. Measurements were performed in quintuplicates and repeated three times.

2.9 Chemotaxis assay

Measurement of the chemotactic responses elicited by the VUV treated samples took place in a two chamber multichannel capillary assay described by Kőhidai L., 1995.

Samples were diluted to 0.1 %, 0.01 %, 0.001 %, 0.0001 %, 0.00001 % and 0.000001 % (v/v) in culturing media. Samples were placed in the upper chamber of the chemotaxis assay whereas cells (10^4) were loaded into the lower one. Following 15 min incubation at 28 °C and fixation with 4% formaldehyde (Reanal, Budapest, Hungary) containing PB, the number of positive responder cells were determined using CASY TT cell counter (Innovatis-Roche, Rotkreuz, Switzerland). Control runs using pure culturing media in the upper chamber served as base for the normalization of cell numbers. The obtained ratio was designated as Chemotaxis Index (Chtx. Ind.). Measurements were carried out in quadruplicates.

2.10 Statistical evaluation

Statistical evaluation of both bioassays was performed using Origin8Pro software. Significance was determined by one-way ANOVA. Normality of data was tested by Shapiro-Wilkinson test whereas homogeneity of variances was checked by Levene's test and Brown-Forsythe test using the same software.

3 Results

3.1 The effect of phosphate buffer

In unbuffered solutions the pH of the samples ($[DICL]_0 = 1.0 \times 10^{-4}$ mol L^{-1}) irradiated for more than 300 s was around the pK_a of DICL (4.2) (Huber et al., 2003) and was higher only in the first stage of VUV photolysis. Thus, during the first 300 s of treatment DICL was predominantly present in its dissociated form (Fig. 2). Since the pH of the irradiated solutions prepared in Milli-Q water changed during the experiments and the pH

was demonstrated to influence the toxicity towards *Tetrahymena pyriformis* (Schultz and Burgan, 2003), samples for toxicity and chemotaxis experiments were taken from buffered DICL solution, to eliminate the effect of pH on the test organisms. In this case the pH of the samples varied in the range of 6.9 – 7.2, therefore DICL was present as an anion also in this case.

Since both $H_2PO_4^-$ and HPO_4^{2-} are reported to be $^{\bullet}OH$ scavengers (Garcia-Araya et al., 2010) it is essential to investigate their effect on the DICL degradation kinetics during VUV photolysis. As it is demonstrated by Fig. 3 neither in O_2 saturated nor in deoxygenated solutions significant difference was found between the DICL decay dissolved in pure water or in buffered solutions ($[DICL]_0 = 1.0 \times 10^{-4}$ mol L^{-1}). However, a slight increase of the reaction rate was observed in Milli-Q water in the presence of O_2 after 120 s of irradiation.

During the VUV photolysis of DICL three aromatic by-products (A, B and C) were detected (their chemical structure is presented in Section 3.4). Their formation and transformation was significantly influenced by the media. In solutions containing dissolved O_2 the concentration of the by-products was higher in the presence, while in solutions purged with N_2 in the absence of phosphates (with the exception of by-product A, where no difference could be found) (Fig. 4).

Among aliphatic by-products oxalic and malonic acids could be detected but only in oxygenated solutions. The observation that the pH of the PB free solutions was lower with 0.4-0.7 units in the presence of O_2 (Fig. 2) corresponds to these data. Also in this case aliphatic by-products were found to be produced in higher concentrations in buffered solutions (Fig. 5).

3.2 The effect of dissolved O_2

As it was shown in Fig. 3, dissolved O_2 had no significant effect on the degradation rate of DICL dissolved in PB but it slightly increased it in Milli-Q water after 120 s of irradiation. According to Fig. 6, the concentration of the aromatic by-products reaches their maxima very close to this irradiation interval, after 90 – 150 s.

Dissolved O_2 affected significantly the formation and transformation of by-products: aliphatic acids could be detected only in oxygenated solutions and the concentration of aromatic by-products was higher (with the exception of by-product A, where the relation was opposite) in deoxygenated solutions prepared in Milli-Q water. On the contrary, in PB containing solutions the accumulation of the aromatic by-products was more remarkable in the presence of O_2 (with the exception of by-product C, where no difference could be found) (Fig. 6).

During the degradation of DICL various chlorine containing (and therefore potentially toxic) by-products may form. Thus, the AOX content of the solutions prepared in Milli-Q water ($[DICL]_0 = 1.0 \times 10^{-4}$ mol L^{-1}) were also measured. As Fig. 7 demonstrates, no significant difference was found between the rates of dehalogenation in the presence or in the absence of O_2.

Since prolonged irradiation was needed to degrade the aromatic by-products (1200 – 1500 s), comparing to the time (900 s) needed for the complete transformation of DICL (Fig. 3 – 6), it is not surprising that the TOC content of the solution was pretty high even after 900 s. Although at the beginning of the treatment no significant difference was found between the mineralization rate of DICL dissolved in Milli-Q water in the presence

and in the absence of O_2, after 600 s (*i.e.* the almost complete transformation of DICL, Fig. 3) the essential role of O_2 became obvious (Fig. 8). After 2 h of VUV photolysis the almost total mineralization of DICL was observed in oxygenated solutions, while under deoxygenated conditions nearly 55% of the initial TOC content of the solution was detected using the same treatment time.

3.3 The effect of the initial DICL concentration

Increasing the $[DICL]_0$ in oxygenated Milli-Q water the decrease of the *k'* value was observed (Fig. 9).

3.4 The chemical structure of the aromatic by-products

According to the HPLC-MS results suggestions could be made for the chemical structures of the aromatic by-products. Using the negative ion mode DICL was observed with an *m/z* value of 294 with two isotope peaks at 296 and 298, regarding to the change of one or two ^{35}Cl to ^{37}Cl. The *m/z* value of by-product A was found to be 310 with two isotope peaks at 312 and 314, suggesting that also this compound contains two Cl atoms. Since the difference between this *m/z* value and the *m/z* value of DICL is 16 and the UV absorbance spectrum of by-product A is very similar to that of DICL (Fig. 10), it is very likely that by-product A is a hydroxylated derivative of DICL.

Hydroxylation could occur on the aromatic rings, resulting in 5-hydroxydiclofenac (A_1), 3-hydroxydiclofenac (A_2), 3'-hydroxydiclofenac (A_3) or 4'-hydroxydiclofenac (A_4) (Calza et al., 2006; Homlok et al., 2011; Landsdorp et al., 1990), on the second carbon

atom of the acetic acid side chain (A_5) or on the nitrogen atom (A_6) (Fig. 11). Among these, 5-hydroxydiclofenac (A_1) was found in most cases to be formed from DICL.

The *m/z* value of by-product B (258) differed by 36 from the *m/z* value of DICL (294) and in this case only one isotope peak (of 260) could be detected. These results and the obvious difference between the UV absorbance spectrum of this compound and DICL (Fig. 10) suggested that in this case HCl elimination occurred and 1-(8-chlorocarbazolyl)acetic acid (Fig. 11, B) was formed, which is a well-known UV-photolytic and photocatalytic degradation product of DICL (Martinez et al., 2011; Moore et al., 1990; Petrovic and Barcelo, 2007).

The *m/z* value of by-product C (240) differed by 18 from the *m/z* value of by-product B (258). In this case no isotope peaks were detected and the UV absorbance spectrum of this compound showed conspicuous similarities with that of by-product B (Fig. 10). Therefore, it is likely that in this case the substitution of the Cl atom of 1-(8-chlorocarbazolyl)acetic acid occurred with an OH group to yield 1-(8-hydroxycarbazolyl)acetic acid, in accordance with the literature (Martinez et al., 2011; Moore et al., 1990; Petrovic and Barcelo, 2007) (Fig. 11, C).

3.5 Cell biological effects of VUV treated samples on the ciliate *Tetrahymena*

Since both direct phototransformation of PhACs in water bodies and advanced oxidation processes lead to the formation of complex mixtures of transformation products, these later should be taken into account when assessing environmental risk of the parent compounds or evaluating efficiency of treatment technologies (Escher and Fenner, 2011; Fatta-Kassinos et al., 2011). With respect to this, in our present work we studied the cell

biological effects of whole VUV treated samples on the proliferation and migratory behavior of the ciliate *Tetrahymena*. Though not yet standardized as a model organism, *Tertahymena* is a highly relevant subject since it is a member of the protozoan trophic level where bioaccumulation of micropollutants having relatively high (>3) log $K_{o/w}$ value, such as DICL, might take place (Gerhardt et al., 2010; Sanderson et al., 2003). Moreover being a member of fresh water biota its relevance may be more obvious than that of marine species such as *V. ficheri* or *A. salina* (Fatta-Kassinos et al., 2011). On the other hand the study of Andreozzi et al., 2004 reported that H_2O_2/UV photolysis of a mixture of PhACs including DICL and quinolone antibiotics resulted in the reduction of toxicity towards algae but not to protozoa stressing out the importance of taking the protozoon trophic levels into account as well.

Proliferation inhibiting effect of untreated sample ($2.5 \cdot 10^{-5}$ mol L^{-1} DICL in PB) was approx. 13%. That was in accordance with our previous results (Láng and Kőhidai, 2012) according to which about 15% proliferation inhibition was expected at this concentration level of DICL. Treated samples taken at definite time of irradiation had slight but significant proliferation inhibiting effect exhibiting different time courses in the case of O_2 saturated or deoxygenated conditions (Fig. 8). Based on the differences between the two conditions regarding the evolution of the time dependent toxicity of 25 % (v/v) diluted samples, three phases could be distinguished: i) in case of 0 s – 300 s of irradiation of oxygenated samples the slight initial inhibition increased to ca. 25% (sample irradiated for 90 s), then returned to its initial level, whereas in case of the deoxygenated condition inhibitory effect decreased to almost 0 % (after 90 s), then returned to the initial value; ii) for samples treated for 600 s – 1800 s inhibition stagnated

around 25 – 30 % in case of both conditions, with a slightly stronger inhibition elicited by the O_2 saturated samples; iii) for samples irradiated for 2400 – 3600 s under oxygenated condition a clear decreasing tendency could be observed in the inhibitory potential reaching only 4% at 3600 s, whereas in case of samples purged with N_2 no important change in the strength of inhibition could be observed. Similar time course but weaker effects were observed for 5 % (v/v) diluted samples, while in the case of 1 % (v/v) samples significant effects were observed only in 2 or 3 samples for O_2 saturated and N_2 purged conditions, respectively (data presented in Tables S1 and S2).

In addition to testing proliferation inhibiting effect of treated samples, their impact on the migratory response of *Tetrahymena* was also tested in sublethal concentrations. The use of such behavioral assays might be advantageous because behavioral changes like avoidance reaction can be, in the most cases, more sensitive and less time consuming indicators of a pollutant's biological impact than acute or chronic toxicity assays (Reinecke et al., 2002). The chemotactic response of *Tetrahymena* spp. has been proposed by several authors as an indicator during the evaluation of water and soil contamination (Gerhardt et al., 2010).

Untreated samples exhibited strong chemorepellent character in 1 % (v/v) dilution (Chtx. Ind. = 50.0 % ± 7.0%) and preserved this character in the whole concentration range studied (47.6 % ± 2.9 % < Chtx. Ind. < 79.0 % ± 6.0 %) (data shown in Tables S3 and S4). This was in agreement with the previous results described by Láng and Kőhidai, 2012 where the chemorepellent effect of DICL was reported in a wide concentration range, though solvents used in the two studies differ (culturing media *vs.* PB). Similarly, treated samples acted predominantly as chemorepellents. For both O_2 saturated and

deoxygenated conditions all samples at 1 % (v/v) dilution elicited negative chemotactic response (Chtx. Ind. ranged from 48.0 % ± 3.0 % to 84.0 % ± 1.0 %) except the neutral behavior of the samples irradiated for 150 s and 2400 s under O_2 and for 1500 s sample under N_2 purged conditions (Fig. 12). Although the very strong initial chemorepellent character decreased over the time, even samples taken after 3000 s or 3600 s of irradiation elicited marked negative chemotactic response for both O_2 and N_2 purged conditions. However, no obvious trend in the evolution of the irradiation time – chemotactic effect curve could be observed for either condition, instead non-linear multiphase curves were found. The proportion of significantly chemorepellent samples decreased in case of both oxygenated and deoxygenated conditions in parallel with the increase of the dilution factor (data shown in Tables S3 and S4).

4 Discussion

4.1 The effect of phosphate buffer

Although both $H_2PO_4^-$ and HPO_4^{2-} react with $^{\bullet}OH$ (2, 3), their reaction rate constants: $k_{H_2PO_4^-}$ (Anbar and Neta, 1967; Maruthamuthu and Neta, 1978) and $k_{HPO_4^{2-}}$ (Black and Hayon, 1970; Garcia-Araya et al., 2010; Maruthamuthu and Neta, 1978) are two – six orders of magnitude lower than the k_{DICL}. Therefore, their reaction rates with $^{\bullet}OH$ ($r_{H_2PO_4^-}$ and $r_{HPO_4^{2-}}$) are significantly lower than that of DICL (r_{DICL}, 4 – 9). Thus, the majority of $^{\bullet}OH$ is likely to react with DICL instead of with $H_2PO_4^-$ or HPO_4^{2-}. Note that at the beginning the photolysis the actual concentrations of DICL, $H_2PO_4^-$ and HPO_4^{2-} ([DICL], [HPO_4^{2-}] and [$H_2PO_4^-$], respectively) can be considered roughly equal to their initial concentrations.

$$HPO_4^{2-} + {}^{\bullet}OH \rightarrow HPO_4^{\bullet -} + OH^- \qquad k_{HPO_4^{2-}} = 1.5 \times 10^5 - 5 \times 10^6\ mol^{-1}\ L\ s^{-1} \quad (2)$$

$$H_2PO_4^- + {}^{\bullet}OH \rightarrow H_2PO_4^{\bullet} + OH^- \qquad k_{H_2PO_4^-} = 2 \times 10^4 - 1 \times 10^7\ mol^{-1}\ L\ s^{-1} \quad (3)$$

$$\frac{r_{DICL}}{r_{HPO_4^{2-}}} = \frac{k_{DICL} \times [{}^{\bullet}OH] \times [DICL]}{k_{HPO_4^{2-}} \times [{}^{\bullet}OH] \times [HPO_4^{2-}]} \quad (4)$$

$$\frac{0.6 \times 10^{10} mol^{-1} Ls^{-1} \times 1.0 \times 10^{-4} mol \sum L^{-1}}{5 \times 10^6 mol^{-1} Ls^{-1} \times 1.9 \times 10^{-3} molL^{-1}} < \frac{r_{DICL}}{r_{HPO_4^{2-}}} < \frac{2.4 \times 10^{10} mol^{-1} Ls^{-1} \times 1.0 \times 10^{-4} molL^{-1}}{0.15 \times 10^6 mol^{-1} Ls^{-1} \times 1.9 \times 10^{-3} molL^{-1}} \quad (5)$$

$$63 < \frac{r_{DICL}}{r_{HPO_4^{2-}}} < 8421 \quad (6)$$

$$\frac{r_{DICL}}{r_{H_2PO_4^-}} = \frac{k_{DICL} \times [{}^{\bullet}OH] \times [DICL]}{k_{H_2PO_4^-} \times [{}^{\bullet}OH] \times [H_2PO_4^-]} \quad (7)$$

$$\frac{0.6 \times 10^{10} mol^{-1} Ls^{-1} \times 1.0 \times 10^{-4} molL^{-1}}{1 \times 10^7 mol^{-1} Ls^{-1} \times 1.1 \times 10^{-3} molL^{-1}} < \frac{r_{DICL}}{r_{H_2PO_4^-}} < \frac{2.4 \times 10^{10} mol^{-1} Ls^{-1} \times 1.0 \times 10^{-4} molL^{-1}}{2 \times 10^4 mol^{-1} Ls^{-1} \times 1.1 \times 10^{-3} molL^{-1}} \quad (8)$$

$$55 < \frac{r_{DICL}}{r_{H_2PO_4^-}} < 109091 \quad (9)$$

The negligible difference, which was found between the degradation rate of DICL in Milli-Q water or in PB (Fig. 3) might be attributed to the above findings.

Although the *k* values of the reactions of the aromatic by-products with ${}^{\bullet}OH$ are not known, they are most probably in the same order of magnitude as k_{DICL} due to the structural similarities of these compounds and the non-selectivity of ${}^{\bullet}OH$. Therefore, the differences between the accumulation and decomposition rates of the by-products in the presence and absence of phosphates (Figs. 4, 5) may be caused by the different pH of the solutions.

The concentration of by-products A–C reached their maxima between 90 – 180 s (Fig. 4a, with the exception of by-product C in PB), which corresponds to the observation that the rate of DICL degradation (in O_2 saturated Milli-Q water) increased slightly after 120 s of irradiation (Fig. 3), where these by-products started to decompose. This could suggest that the increased concentration of the by-products reduces the concentration of reactive radicals and therefore the efficiency of DICL transformation.

In deoxygenated solutions, no PB caused inhibition of DICL degradation was found (Fig. 3). Moreover, the accumulation of the aromatic by-products was lower in the presence of PB. In this case the radicals formed from $H_2PO_4^-$ and HPO_4^{2-} ($H_2PO_4^\bullet$ and $HPO_4^{\bullet-}$) might contribute to the transformation of the by-products, since the second order reaction rates of these radicals with some organic compounds were determined to be in the range of $10^7 – 10^8$ mol^{-1} L s^{-1} (Nakashima and Hayon, 1970). The effect of PB in oxygenated solutions will be discussed in the next section.

4.2 The effect of dissolved O_2

Dissolved O_2 scavenges $H^\bullet$ resulting in hydroperoxyl radicals ($HO_2^\bullet$) and their conjugate base-pair, in superoxide radical ions ($O_2^{\bullet-}$) (10, 11) (Gonzalez et al., 2004). These oxygen containing radicals might also contribute to the degradation of organic contaminants.

$H^\bullet + O_2 \rightarrow HO_2^\bullet$ $\quad k_{10} = 1.2 \times 10^{10}$ mol^{-1} L s^{-1} (Buxton et al., 1988) (10)

$HO_2^\bullet \rightleftharpoons H^+ + O_2^{\bullet-}$ $\quad pK_a = 4.8$ (Bielski et al., 1985) (11)

Since the pH of the solutions in the absence of PB decreased below the pK_a of $HO_2^\bullet$ after 300 s of irradiation (Fig. 2), in oxygenated solutions the dominance of $HO_2^\bullet$ above $O_2^{\bullet-}$ should be taken into consideration, using longer reaction times.

No significant difference was found between the initial degradation rates of DICL in the presence or in the absence of O_2 (Fig. 3). The only exception is the prolonged irradiation of solutions prepared in Milli-Q water, which might be attributed to the raise of H_2O_2 and $HO_2^{\bullet}$ concentration, which is reported to elevate during the degradation of organic contaminants (Arany et al., 2012; Azrague et al., 2005; Robl et al., 2012). On the one hand, the similarity between the degradation curves in oxygenated (the dominant radicals being $HO_2^{\bullet}$ and $^{\bullet}OH$) and deoxygenated solutions (the dominant species being $H^{\bullet}$ and $^{\bullet}OH$) would suggest that $H^{\bullet}$ and $HO_2^{\bullet}$ react with DICL with similar rate constants. On the other hand, the slight increase of the DICL transformation rate after 120 s of irradiation in O_2 saturated Milli-Q water would refer to that the effect of $HO_2^{\bullet}$ is considerable only in its higher concentration.

$HO_2^{\bullet}/O_2^{\bullet-}$ might also affect the formation and degradation of aromatic by-products. Since in Milli-Q water the accumulation of by-product A was more remarkable in the presence of O_2 while the concentration of by-products B and C was higher in solutions purged with N_2, it is likely that $HO_2^{\bullet}$ contribute to the formation of the former and the transformation of the latter two compounds. The reactions of aromatic by-products with $^{\bullet}OH$ and $HO_2^{\bullet}/O_2^{\bullet-}$ (with unknown *k* values) might also contribute to the differences between the measured concentrations of by-products A–C.

If $^{\bullet}OH$ reacts with organic compounds (*e.g.* with DICL or its degradation by-products) through hydrogen abstraction or addition reactions, carbon centered radicals ($R^{\bullet}$) form (Gonzalez et al., 2004; Legrini et al., 1993; Sosnin et al., 2006), which are scavenged in oxygenated solutions by O_2 resulting in peroxyl radicals ($ROO^{\bullet}$). These radicals might also contribute to DICL degradation and could result in the increased transformation rate

observed after 120 s of irradiation in Milli-Q water. The formation of aliphatic acids could be described by the reactions of $ROO^{\bullet}$ resulting in the cleavage of the aromatic rings (Getoff, 1996; Oppenländer, 2003).

In buffered solutions the pH was found to be above the pK_a of $HO_2^{\bullet}$ (Fig. 2). This radical is therefore present in form of its conjugate base-pair under these conditions. The similarity of DICL degradation curves in the presence and absence of O_2 in buffered solutions (Fig. 3) might be explained with the low reactivity of $O_2^{\bullet-}$ towards DICL even at higher concentrations (*viz.* using prolonged irradiation).

Since in oxygenated solutions the concentration of aromatic by-products was higher in the presence of PB (where $HO_2^{\bullet}/O_2^{\bullet-}$ is mainly present in the form of $O_2^{\bullet-}$), compared to the samples prepared in Milli-Q water (where $HO_2^{\bullet}/O_2^{\bullet-}$ is mainly present in the form of $HO_2^{\bullet}$) (Fig. 4a), the lower DICL degradation rate in the presence of phosphates can be interpreted with the probably lower reaction rate of DICL and its by-products with $O_2^{\bullet-}$, compared to their reactions with $HO_2^{\bullet}$.

In PB the difference between the reactions of $ROO^{\bullet}$ and $R^{\bullet}$ (formed from the by-products in oxygenated and deoxygenated solutions, respectively) with $H_2PO_4^-$, HPO_4^{2-}, $H_2PO_4^{\bullet}$ and $HPO_4^{\bullet-}$ might result in the difference between the accumulation of aromatic by-products in the presence and absence of O_2 (Fig. 6b).

The similar degradation rate of DICL in oxygenated and deoxygenated solutions prepared in Milli-Q water and the observation that by-product A was detected in higher concentration in the presence of O_2 while by-products B and C in solutions purged with N_2, might explain the negligible difference between the dehalogenation efficiency depending on the concentration of dissolved O_2 (Fig. 7).

However, significant difference was found between the rate of mineralization in the presence and absence of O_2 (Fig. 8). Since even the aliphatic acids were almost completely degraded after 2 h of VUV irradiation in oxygenated solutions (Fig. 5), the almost total diminution of the TOC content suited our expectations. Although aliphatic acids could not be detected in solutions purged with N_2, nearly 55% of the initial TOC content of the solution was detected even after 2 h of treatment. This would suggest that in deoxygenated solutions, some undetected recalcitrant by-products are formed. Therefore, the essential role of dissolved O_2 during the effective decontamination of DICL containing solutions should be underlined.

In the absence of O_2 the recombination of the $R^{\bullet}$ formed in the reaction of DICL and $^{\bullet}OH$ is very likely and may result in dimers and oligomers of DICL, analoguously to the transformation of other organic contaminants (Gonzalez et al., 2004; Sosnin et al., 2006). The degradation of these compounds is much more difficult than that of the original molecule, which could explain the low efficiency of TOC diminution in deoxygenated solutions (Fig. 8).

In the presence of dissolved O_2 the recombination of the $ROO^{\bullet}$ may happen. The formation of tetroxides could be supported by the fact that the concentration of the detected aliphatic acids reached their maxima around 3000 s although both DICL and the measured aromatic by-products transformed completely after 1500 s of irradiation (Figs. 3–6). Thus, the source of malonic and oxalic acids should be different from DICL or from by-products A–C, *e.g.* they could arise from some tetroxides. The higher mineralization rate in this case (Fig. 8) might be explained by the different transformation pathways of tetroxides (*e.g. via* the Russell mechanism) (von Sonntag and Schuchmann, 1991).

4.3 The effect of the initial DICL concentration

If $[DICL]_0$ is fixed, the pseudo first-order approach is suitable to describe the degradation kinetics of the VUV photolysis of our model compound. However, $[DICL]_0$ influences the value of [$^{\bullet}$OH]: the increase of the former initiates the decrease of the latter, since more $^{\bullet}$OH are involved in their reactions with DICL. Thus, our observation, that the *k'* (= $k \times$ [$^{\bullet}$OH]) values decrease with the increase of $[DICL]_0$ (Fig. 9) can be explained with the decrease of [$^{\bullet}$OH] along with the constant value of *k*.

4.4 The formation of the aromatic by-products

Since $^{\bullet}$OH is an electrophilic radical, it usually attacks on the electron-dense sites of the aromatic rings, *e.g.* on the 5, 3, 3' and 4' carbon atoms of DICL. Analogously to the proposed mechanisms regarding the formation of 5-hydroxydiclofenac in $^{\bullet}$OH initiated reactions (Garcia-Araya et al., 2010; Homlok et al., 2011; Sein et al., 2008), Fig. 13 depicts the $^{\bullet}$OH addition to DICL in the 3 position to result in a hydroxycyclohexadienyl type radical. After the addition of an O_2 molecule and the elimination of a $HO_2^{\bullet}$ 3-hydroxydiclofenac might be formed. Formation of hydroxylated by-products is not probable in the absence of dissolved O_2. The fact that by-product A was detected in significantly lower concentration both in the presence and absence of PB (Fig. 6b) in deoxygenated solutions compared to the O_2 saturated conditions, supports this assumption.

Our results suggest that O_2 addition and HCl elimination might be competitive processes regarding the transformation of the hydroxycyclohexadienyl type radical. The latter one

could result in ring closure and after a reaction with a $R^{\bullet}$ by-product B might be formed. Similar mechanism might be proposed for the formation of 1-(8-chlorocarbazolyl)acetic acid (B) as a result of the reaction of DICL with $H^{\bullet}$, therefore by-product B might be formed also in deoxygenated solutions (Fig. 13).

After the addition of a $^{\bullet}OH$ to by-product B in O_2 saturated solutions again a competition might arise between $^{\bullet}Cl$ elimination (to result in by-product C) and O_2 addition. Naturally, the latter process cannot be realized in deoxigenated solutions (Fig. 13).

4.5 Cell biological effect of VUV treated samples

In the present work, the concept of the biological activity evaluation was to use a new, relatively simple and rapid, high-throughput, yet highly sensitive screening assay combination, rather than performing a time consuming and labor intensive effect directed analysis of samples. Results about the proliferation inhibiting and migration influencing effects of VUV treated samples (Figs. 8 and 12) reflected the chemical transformation of DICL and the formation of complex mixtures composed of several by-products. Depending on the operating condition applied, irradiation time-proliferation inhibition curves of different shapes were obtained in accordance with the alterations between the two conditions (oxygenated or deoxygenated) regarding the amount of produced by-products and the diminution of the TOC content. The initial enhancement (until 90 s) of the inhibitory potential under O_2 saturated condition in contrast to the slightly decreasing tendency of the N_2 purged condition might be correlated to the significantly higher amount of by-product A formed using O_2. These results are in accordance with the findings of gamma radiolysis, *viz.* by-products formed during oxidative conditions are

more toxic towards *Vibrio fischeri* than those detected using reductive conditions (Yu, 2013). On the other hand, the stagnating toxicity observed using N_2 for samples irradiated for 2400 s – 3600 s in contrast to the decrease of the inhibition in samples containing O_2 may be explained by the lower mineralization rate in case of using N_2 as purge gas. As Fig. 8 shows, *ca* 25 % mineralization was reached after 3000 s of irradiation using N_2 and even after 7000 s of irradiation mineralization did not exceeded approx. 40%. Moreover, in this phase of irradiation some di- and polymer by-products might be formed that could not be detected under the applied analytical methods (Gonzalez-Rey and Bebianno, 2012; Sosnin et al., 2006); however, they can significantly contribute to the mixture toxicity. In the case of O_2 saturated condition a higher mineralization was achieved, 70 % after 3000 s and 75 % after 3600 s of treatment that might be linked to the reduced toxicity of the respective samples. Anyhow, for both of the two conditions no dramatically increased inhibiting effect occurred during the 3600 s irradiation time as it was reported for the direct photolysis (Schmitt-Jansen et al., 2007) or photocatalytic degradation of DICL (Rizzo et al., 2009). In our study the maximal toxicity (about 30 %) was approx. 2 times higher than that of the parent compound whereas the above mentioned publications described 5 or 6 fold stronger toxic potential of transformation product mixtures compared to the parent compound.

To our knowledge no study was performed until know using the chemotactic response as indicator for the biological assessment of samples generated by advanced oxidation processes. Similarly to toxicity profiles, differences in the chemotactic character could be observed depending on the gas applied for purge. In general, transformation product mixtures retained the chemorepellent property of the parent compound DICL (Fig. 12).

However, both cell proliferation and migratory responses might involve multiple potential biological signaling pathways (i.e. different membrane receptors and respective downstream signaling cascades mediated for example by cyclic adenozine monophosphate (c-AMP), cyclic guanozine monophosphate (c-GMP), phosphatidylinositol (3,4,5)-triphosphate (PIP3) or Ca^{2+}). Consequently, further investigations are needed in order to understand the mechanism of action of the individual transformation products as well as their possible interactions in their mixtures.

5 Conclusions

The similarities of the DICL degradation curves in the presence and absence of dissolved O_2 suggest that $H^{\bullet}$ and $HO_2^{\bullet}$ react with DICL with similar reaction rate constants.

Since the presence of phospates affected mostly the formation and degradation of the by-products and influenced only silghtly the transformation of DICL itself, it is very likely that their effect is due to the alteration of the solution pH. The radical scavenging effect of PB seems to be negligible both in oxygenated and deoxygenated solutions.

The contribution of $HO_2^{\bullet}$ to the degradation of DICL or its by-products appears to be significant only if the accumulation of this radical occurs, however the effect of $O_2^{\bullet-}$ seems to be of lower importance.

During the VUV photolysis of DICL some aliphatic acids and three major aromatic by-products (a hydroxilated derivative of DICL – most probably 5-hydroxydiclofenac –, 1-(8-chlorocarbazolyl)acetic acid and 1-(8-hydroxycarbazolyl)acetic acid) could be detected.

Our approach of investigating the biological effects of whole mixtures generated by different time of photoexposure of DICL allowed to take into account also the complex interactions that might occur in these multicomponent mixtures containing numerous transformation products. Using this rapid screening method the impact of different operating conditions on the VUV photolysis of DICL as well as the efficiency of this technology could be evaluated. Moreover, our results suggest that the VUV photolysis coupled to the rapid biological screening of treated samples can also be valuable in the elimination studies of other micropollutants from water matrices.

Acknowledgments

The authors express their gratitude to Dr. Ágota Tóth and Dr. Dezső Horváth (Department of Physical Chemistry and Materials Science, University of Szeged) for their help in the interpretation and the kinetic modelling of the degradation curves. This work was supported by the Swiss Contribution (SH7/2/20).

References

Anbar M, Neta P. A compilation of specific bimolecular rate constants for the reactions of hydrated electrons, hydrogen atoms and hydroxyl radicals with inorganic and organic compounds in aqueous solutions. Int J Appl Radiat Isot 1967; 18: 493–523.

Andreozzi R, Campanella L, Fraysse B, Garric J, Gonnella A, Lo Giudice R, et al. Effects of advanced oxidation processes (AOPs) on the toxicity of a mixture of pharmaceuticals. Water Sci Technol 2004; 50: 23-28.

Arany E, Oppenländer T, Gajda-Schrantz K, Dombi A. Influence of H_2O_2 formed in situ on the photodegradation of ibuprofen and ketoprofen. Curr Phys Chem 2012; 2: 286–293.

Aruoma OI, Halliwell B. The iron-binding and hydroxyl radical scavenging action of anti-inflammatory drugs. Xenobiotica 1988; 18: 459-470.

Azrague K, Bonnefille E, Pradines V, Pimienta V, Oliveros E, Maurette M-T, et al. Hydrogen peroxide evolution during V-UV photolysis of water. Photochem Photobiol Sci 2005; 4: 406–408.

Bernabeu A, Vercher RF, Santos-Juanes L, Simon PJ, Lardin C, Martinez MA, et al. Solar photocatalysis as a tertiary treatment to remove emerging pollutants from wastewater treatment plant effluents. Catal Today 2011; 161: 235-240.

Bielski BHJ, Cabelli DE, Arudi RL, Ross AB. Reactivity of HO_2/O_2^- radicals in aqueous solution. J Phys Chem Ref Data 1985; 14: 1041–1100.

Black ED, Hayon E. Pulse radiolysis of phosphate anions $H_2PO_4^-$, HPO_4^{2-}, PO_4^{3-} and $P_2O_7^{4-}$ in aqueous solutions. J Phys Chem 1970; 74: 3199−3203.

Boreen AL, Arnold WA, McNeill K. Photodegradation of pharmaceuticals in the aquatic environment: A review. Aquat Sci 2003; 65: 320-341.

Buser HR, Poiger T, Muller MD. Occurrence and fate of the pharmaceutical drug diclofenac in surface waters: Rapid photodegradation in a lake. Environ Sci Technol 1998; 32: 3449-3456.

Buxton GV, Greenstock CL, Helman WP, Ross AB. Critical review of rate constants for reactions of hydrated electrons, hydrogen atoms and hydroxyl radicals ($^{\bullet}OH/^{\bullet}O^-$) in aqueous solution. J Phys Chem Ref Data 1988; 17: 513–886.

Calza P, Sakkas VA, Medana C, Baiocchi C, Dimou A, Pelizzetti E, et al. Photocatalytic degradation study of diclofenac over aqueous TiO2 suspensions. Appl Catal, B 2006; 67: 197-205.

Canonica S, Meunier L, von Gunten U. Phototransformation of selected pharmaceuticals during UV treatment of drinking water. Water Res 2008; 42: 121-128.

Daughton CG. Pharmaceutical Ingredients in Drinking Water: Overview of Occurrence and Significance of Human Exposure. In: Halden R, editor. Contaminants of emerging conrcern in the environment: ecological and human health considerations. American Chemical Society, Washington D.C., 2010, pp. 9-68.

Escher BI, Fenner K. Recent advances in environmental risk assessment of transformation products. Environ Sci Technol 2011; 45: 3835-3847.

Fatta-Kassinos D, Vasquez MI, Kümmerer K. Transformation products of pharmaceuticals in surface waters and wastewater formed during photolysis and advanced oxidation processes – Degradation, elucidation of byproducts and assessment of their biological potency. Chemosphere 2011; 85: 693-709.

Garcia-Araya JF, Beltran FJ, Aguinaco A. Diclofenac removal from water by ozone and photolytic TiO2 catalysed processes. J Chem Technol Biotechnol 2010; 85: 798-804.

Gerhardt A, Ud-Daula A, Schramm KW. Tetrahymena spp. (Protista, Ciliophora) as test species in rapid multilevel ecotoxicity tests. Acta Protozool 2010; 49: 271-280.

Getoff N. Radiation-induced degradation of water pollutants - state of the art. Radiat Phys Chem 1996; 47: 581–593.

Gonzalez-Rey M, Bebianno MJ. Does non-steroidal anti-inflammatory (NSAID) ibuprofen induce antioxidant stress and endocrine disruption in mussel Mytilus galloprovincialis? Environ Toxicol Pharmacol 2012; 33: 361-371.

Gonzalez MG, Oliveros E, Wörner M, Braun AM. Vacuum-ultraviolet photolysis of aqueous reaction systems. J Photochem Photobiol, C 2004; 5: 225–246.

Homlok R, Takacs E, Wojnarovits L. Elimination of diclofenac from water using irradiation technology. Chemosphere 2011; 85: 603-608.

Huber MM, Canonica S, Park G-Y, von Gunten U. Oxidation of pharmaceuticals during ozonation and Advanced Oxidation Processes. Environ Sci Technol 2003; 37: 1016–1024.

Khan SJ, Ongerth JE. Modelling of pharmaceutical residues in Australian sewage by quantities of use and fugacity calculations. Chemosphere 2004; 54: 355-367.

Klamerth N, Miranda N, Malato S, Aguera A, Fernandez-Alba AR, Maldonado MI, et al. Degradation of emerging contaminants at low concentrations in MWTPs effluents with mild solar photo-Fenton and TiO2. Catal Today 2009; 144: 124-130.

Kőhidai L. Method for determination of chemoattraction in Tetrahymena pyriformis. Curr Microbiol 1995; 30: 251-253.

Kruithof JC, Kamp PC, Martijn BJ. UV/H2O2 treatment: A practical solution for organic contaminant control and primary disinfection. Ozone: Sci Eng 2007; 29: 273–280.

Landsdorp D, Vree TB, Janssen TJ, Guelen PJM. Pharmacokinetics of rectal diclofenac and its hydroxy metabolites in man. Int J Clin Pharmacol Ther 1990; 28: 298-302.

Láng J, Kőhidai L. Effects of the aquatic contaminant human pharmaceuticals and their mixtures on the proliferation and migratory responses of the bioindicator freshwater ciliate Tetrahymena. Chemosphere 2012; 89: 592-601.

Lapworth DJ, Baran N, Stuart ME, Ward RS. Emerging organic contaminants in groundwater: A review of sources, fate and occurrence. Environ Pollut 2012; 163: 287-303.

Legrini O, Oliveros E, Braun AM. Photochemical processes for water treatment. Chem Rev 1993; 93: 671–698.

Martinez C, Canle M, Fernandez MI, Santaballa JA, Faria J. Aqueous degradation of diclofenac by heterogeneous photocatalysis using nanostructured materials. Appl Catal, B 2011; 107: 110-118.

Maruthamuthu P, Neta P. Phosphate radicals − spectra, acid-base equilibria and reactions with inorganic compounds. J Phys Chem 1978; 82: 710-713.

Meunier L, Canonica S, von Gunten U. Implications of sequential use of UV and ozone for drinking water quality. Water Res 2006; 40: 1864-1876.

Moore DE, Roberts-Thomson S, Zhen D, Duke CC. Photochemical studies on the anti-inflammatory drug diclofenac. Photochem Photobiol 1990; 52: 685–690.

Nakashima M, Hayon E. Rates of reaction of inorganic phosphate radicals in solution. J Phys Chem 1970; 74: 3290–3291.

Oaks JL, Gilbert M, Virani MZ, Watson RT, Meteyer CU, Rideout BA, et al. Diclofenac residues as the cause of vulture population decline in Pakistan. Nature 2004; 427: 630-633.

Oppenländer T. Photochemical purification of water and air. Weinheim: Wiley-VCH, 2003.

Oppenlander T, Schwarzwalder R. Vacuum-UV oxidation (H2O-VUV) with a xenon excimer flow-trough lamp at 172 nm: Use of methanol as actinometer for VUV intensity measurement and as reference compound for OH-radical competition kinetics in aqueous systems. J Adv Oxid Technol 2002; 5: 155-163.

Pal A, Gin KYH, Lin AYC, Reinhard M. Impacts of emerging organic contaminants on freshwater resources: Review of recent occurrences, sources, fate and effects. Sci Total Environ 2010; 408: 6062–6069.

Parij N, Nagy AM, Neve J. Linear and nonlinear competition plots in the deoxyribose assay for determination of rate constants for reaction of nonsteroidal aniinflammatory drugs with hydroxyl radicals. Free Radical Res 1995; 23: 571–579.

Perez-Estrada LA, Maldonado MI, Gernjak W, Aguera A, Fernandez-Alba AR, Ballesteros MM, et al. Decomposition of diclofenac by solar driven photocatalysis at pilot plant scale. Catal Today 2005; 101: 219-226.

Petrovic M, Barcelo D. LC-MS for identifying photodegradation products of pharmaceuticals in the environment. Trends Anal Chem 2007; 26: 486-493.

Poiger T, Buser HR, Muller MD. Photodegradation of the pharmaceutical drug diclofenac in a lake: Pathway, field measurements, and mathematical modeling. Environ Toxicol Chem 2001; 20: 256-263.

Ratola N, Cincinelli A, Alves A, Katsoyiannis A. Occurrence of organic microcontaminants in the wastewater treatment process. A mini review. J Hazard Mater 2012; 239–240: 1-18.

Reinecke AJ, Maboeta MS, Vermeulen LA, Reinecke SA. Assessment of Lead Nitrate and Mancozeb Toxicity in Earthworms Using the Avoidance Response Bull Environ Contam Toxicol 2002; 68: 779-786.

Rizzo L, Meric S, Kassinos D, Guida M, Russo F, Belgiorno V. Degradation of diclofenac by TiO(2) photocatalysis: UV absorbance kinetics and process evaluation through a set of toxicity bioassays. Water Res 2009; 43: 979-988.

Robl S, Worner M, Maier D, Braun AM. Formation of hydrogen peroxide by VUV-photolysis of water and aqueous solutions with methanol. Photochem Photobiol Sci 2012; 11: 1041-1050.

Sanderson H, Johnson DJ, Wilson CJ, Brain RA, Solomon KR. Probabilistic hazard assessment of environmentally occurring pharmaceuticals toxicity to fish, daphnids and algae by ECOSAR screening. Toxicol Lett 2003; 144: 383-395.

Santos LHMLM, Araújo AN, Fachini A, Pena A, Delerue-Matos C, Montenegro MCBSM. Ecotoxicological aspects related to the presence of pharmaceuticals in the aquatic environment. J Hazard Mater 2010; 175: 45-95.

Schmitt-Jansen M, Bartels P, Adler N, Altenburger R. Phytotoxicity assessment of diclofenac and its phototransformation products. Anal Bioanal Chem 2007; 387: 1389-1396.

Schultz TW, Burgan JT. pH-stress and toxicity of nitrophenols to Tetrahymena pyriformis. Bull Environ Contam Toxicol 2003; 71: 1069-1076.

Sein MM, Zedda M, Tuerk J, Schmidt TC, Golloch A, von Sonntao C. Oxidation of diclofenac with ozone in aqueous solution. Environ Sci Technol 2008; 42: 6656-6662.

Sosnin EA, Oppenländer T, Tarasenko VF. Applications of capacitive and barrier discharge excilamps in photoscience. J Photochem Photobiol, C 2006; 7: 14–163.

Ternes TA. Occurrence of drugs in German sewage treatment plants and rivers. Water Res 1998; 32: 3245–3260.

Vogna D, Marotta R, Napolitano A, Andreozzi R, d'Ischia M. Advanced oxidation of the pharmaceutical drug diclofenac with UV/H_2O_2 and ozone. Water Res 2004; 38: 414-422.

von Sonntag C, Schuchmann H-P. The elucidation of peroxyl radical reactions in aqueous solution with the help of radiation-chemical methods. Angew Chem, Int Ed 1991; 30: 1229–1253.

Vulliet E, Cren-Olivé C, Grenier-Loustalot M-F. Occurrence of pharmaceuticals and hormones in drinking water treated from surface waters. Environ Chem Lett 2011; 9: 103-114.

Yu H, Nie E, Xu J, Yan S, Cooper WJ, Song W. Degradation of diclofenac by advanced oxidation and reduction processes: Kinetic studies, degradation pathways and toxicity assessments. Water Res 2013; 47: 1909–1918.

Zhang Y, Geißen S-U, Gal C. Carbamazepine and diclofenac: Removal in wastewater treatment plants and occurrence in water bodies. Chemosphere 2008; 73: 1151-1161.

1 Zwiener C, Frimmel FH. Short-term tests with a pilot sewage plant and biofilm reactors
2 for the biological degradation of the pharmaceutical compounds clofibric acid,
3 ibuprofen, and diclofenac. Sci Total Environ 2003; 309: 201-211.

Figure captions

Fig. 1. The scheme of the photochemical apparatus 1: power supply; 2: teflon packing ring; 3: xenon excimer lamp; 4: reactor; 5: peristaltic pump; 6: reservoir; 7: magnetic stirrer; 8: flow meter; 9: oxygen or nitrogen bottle and 10: thermostat

Fig. 2. The pH of DICL containing solutions ($[DICL]_0 = 1.0 \times 10^{-4}$ mol L^{-1}) during VUV photolysis

Fig. 3. The effect of PB as well as dissolved O_2 on the VUV photolysis of DICL ($[DICL]_0 = 1.0 \times 10^{-4}$ mol L^{-1})

Fig. 4. The effect of PB on the formation and transformation of a) by-product A in oxygenated and b) by-product B in deoxygenated solutions during the VUV photolysis of DICL ($[DICL]_0 = 1.0 \times 10^{-4}$ mol L^{-1})

Fig. 5. The effect of PB on the formation and transformation of malonic and oxalic acids in oxygenated solutions during the VUV photolysis of DICL ($[DICL]_0 = 1.0 \times 10^{-4}$ mol L^{-1})

Fig. 6. The effect of dissolved O_2 on the formation and transformation of by-product C during the VUV photolysis of DICL ($[DICL]_0 = 1.0 \times 10^{-4}$ mol L^{-1}) dissolved in a) Milli-Q water and b) in PB

Fig. 7. The effect of dissolved O_2 on the dehalogenation during the VUV photolysis of DICL ($[DICL]_0 = 1.0 \times 10^{-4}$ mol L^{-1}) dissolved in Milli-Q water

Fig. 8. The effect of dissolved O_2 on the mineralization and on the degree of proliferation inhibition of *Tetrahymena* during the VUV photolysis of DICL ($[DICL]_0 = 1.0 \times 10^{-4}$ mol L^{-1}) dissolved in Milli-Q water. Significance levels correspond to: x: $p<0.05$; y: $p<0.01$; z: $p<0.001$.

Fig. 9. The effect of the initial DICL concentration on the apparent reaction rate constant of the VUV photolysis of oxygenated solutions prepared in Milli-Q water

Fig. 10. The UV absorbance spectra of DICL, by-products A, B and C

Fig. 11. The possible chemical structures of by-products A, B and C

Fig. 12. Migratory responses of *Tetrahymena* elicited by the VUV treated samples (1 v/v %) generated using either O_2 saturated ("O_2") or deoxygenated ("N_2") condition. Significance levels are: $x<0.05$; $y<0.01$; $z<0.001$

Fig. 13. The possible formation pathway of by-products A_2, B and C

Supplementary Material

Table S1. Concentration and time dependent proliferation inhibiting effect of VUV treated samples taken from O_2 saturated solutions and the standard errors of the means (SE)

	1 v/v%		5 v/v%		25 v/v%	
t (s)	Cell number (%)	SE (%)	Cell number (%)	SE (%)	Cell number (%)	SE (%)
0	105.3	4.2	89.3^{x}	3.9	87.6^{x}	4.2
10	107.2	4.0	88.8^{x}	4.4	84.7^{x}	4.1
20	101.1	2.1	89.0^{x}	4.7	82.5^{y}	4.3
40	105.5	1.9	85.6^{x}	3.9	78.0^{z}	3.7
90	98.1	2.4	83.0^{y}	2.4	75.8^{z}	4.0
150	100.8	2.0	85.3^{x}	1.6	82.1^{y}	3.4
300	98.0	2.8	87.0^{x}	2.8	86.0^{x}	2.8
600	97.1	2.7	91.5	2.9	76.0^{z}	1.6
900	96.0	1.8	88.2^{x}	2.4	82.9^{y}	1.5
1200	89.9^{x}	2.2	83.0^{y}	1.7	73.5^{z}	2.5
1500	87.2^{x}	2.4	83.6^{y}	4.1	67.9^{z}	1.9
1800	96.2	2.3	93.3	1.6	80.6^{y}	3.1
2400	97.4	2.2	86.6^{x}	3.1	82.9^{y}	2.9
3000	95.0	2.2	92.6	2.3	90.6	4.5
3600	96.2	2.1	94.2	2.6	92.4	2.4

significance levels are: x<0.05; y<0.01; z<0.001

Table S2. Concentration and time dependent proliferation inhibiting effect of VUV treated samples taken from O_2 deprived solutions and the standard error of the means (SE)

	1 v/v%		5 v/v%		25 v/v%	
t (s)	Cell number (%)	SE (%)	Cell number (%)	SE (%)	Cell number (%)	SE (%)
0	105.3	4.2	89.3^{x}	3.9	87.6^{x}	4.2
10	91.5	2.4	89.9^{x}	1.8	90.7^{x}	2.1
20	92.8	4.7	89.5^{x}	3.6	88.9^{x}	3.2
40	96.5	4.6	87.2^{x}	2.9	88.0^{x}	2.6
90	96.3	4.5	96.1	3.0	96.0	3.4
150	100.4	5.6	88.8^{x}	2.7	93.3	2.6
300	98.0	3.3	98.9	2.9	89.2^{x}	1.6
600	91.3	4.4	80.5^{y}	1.8	80.6^{z}	3.0
900	94.0	3.5	90.7^{x}	3.7	85.1^{y}	2.5
1200	84.4^{y}	2.4	78.0^{z}	1.9	77.2^{z}	3.4
1500	95.0	2.7	81.7^{y}	2.5	74.6^{z}	3.0
1800	96.1	2.4	88.0^{x}	2.7	80.9^{z}	2.9
2400	90.9	2.8	83.9^{y}	4.2	78.6^{z}	2.7
3000	87.1^{x}	3.7	86.9^{x}	1.1	72.3^{z}	2.8
3600	86.6^{x}	3.7	83.9^{y}	2.5	77.2^{z}	3.0

significance levels are: $x<0.05$; $y<0.01$; $z<0.001$

Tables S3. Migratory responses of *Tetrahymena* elicited by VUV treated samples taken at O_2 saturated conditions and the standard errors of the means (SE)

	0.0001 v/v%		0.001 v/v%		0.01 v/v%		0.1 v/v%		1 v/v%	
t (s)	Chtx. Ind. (%)	SE (%)	Chtx. Ind. (%)	SE (%)	Chtx. Ind. (%)	SE (%)	Chtx. Ind. (%)	SE (%)	Chtx. Ind. (%)	SE (%)
0	79.0^{y}	6.0	54.0^{z}	2.6	70.2^{z}	6.3	47.6^{z}	2.9	50.0^{z}	7.0
10	94.9	7.6	86.1^{x}	10.9	97.7	12.5	63.0^{z}	7.5	74.6^{y}	3.5
20	88.1^{x}	6.4	80.6^{x}	5.0	61.7^{z}	4.1	100.2	3.9	92.1	8.0
40	90.3	5.8	91.9	8.0	94.6	5.6	85.4^{x}	8.3	63.7^{z}	4.2
90	135.2^{y}	7.7	91.4	2.4	92.3	7.8	74.6^{y}	1.8	80.7^{x}	7.3
150	133.3^{x}	13.4	121.1	10.1	79.2^{y}	2.6	75.7^{y}	2.1	97.1	16.6
300	107.5	6.1	122.6^{x}	6.0	106.7	7.6	71.3^{y}	7.4	72.5^{y}	3.8
600	87.0_{x}	4.9	93.0	6.5	73.5^{y}	2.4	68.2^{y}	1.8	99.9	6.0
900	98.4	6.0	96.9	2.9	87.3^{x}	6.3	95.0	10.4	77.5^{y}	6.0
1200	122.0^{x}	8.3	136.0^{y}	2.0	83.5^{x}	7.2	114.9	12.8	55.0^{z}	5.5
1500	95.3	3.8	70.5^{y}	7.5	105.6	8.4	59.4^{z}	3.4	89.3	10.9
1800	117.7^{x}	5.8	82.3^{x}	5.8	92.6	7.3	71.5^{y}	4.8	79.9^{y}	8.5
2400	104.4	8.9	128.5^{x}	12.3	80.3^{x}	6.2	87.2^{x}	6.9	96.4	2.0
3000	87.6x	4.0	85.1^{x}	9.8	79.8^{x}	5.4	66.8^{y}	8.9	75.5^{y}	5.6
3600	122.2	13.6	93.7	19.9	83.5^{x}	10.4	59.9^{y}	5.0	55.3^{z}	6.2

significance levels are: x<0.05; y<0.01; z<0.001

Tables S4. Migratory responses of *Tetrahymena* elicited by VUV treated samples taken at deoxygenated conditions and the standard errors of the means (SE)

	0.0001 v/v%		0.001 v/v%		0.01 v/v%		0.1 v/v%		1 v/v%	
t (s)	Chtx. Ind. (%)	SE (%)	Chtx. Ind. (%)	SE (%)	Chtx. Ind. (%)	SE (%)	Chtx. Ind. (%)	SE (%)	Chtx. Ind. (%)	SE (%)
0	79.0^{y}	6.0	54.0^{z}	2.6	70.2^{z}	6.3	47.6^{z}	2.9	50.0^{z}	7.0
10	84.0^{y}	5.5	85.0^{x}	6.0	76.0^{z}	5.0	96.0	6.5	76.0^{y}	3.5
20	138.0^{y}	7.0	110.0	9.5	121.0^{x}	2.5	99.0	13.0	69.0^{z}	3.5
40	102.0	5.0	117.0	6.0	89.0	8.0	65.0^{z}	4.0	84.0^{y}	1.0
90	72.0^{z}	5.0	69.0^{z}	5.5	65.0^{z}	6.0	59.0^{z}	3.5	48.0^{z}	3.0
150	90.0	7.5	100.0	5.0	77.0^{z}	2.5	81.0^{x}	4.0	68.0^{z}	2.5
300	95.1	3.2	76.5^{y}	9.1	85.2^{x}	9.4	86.5^{x}	6.5	80.4^{x}	5.5
600	107.1	6.5	102.9	3.8	92.4	10.7	89.3	11.2	61.8^{z}	3.4
900	90.9	5.1	89.2	5.6	81.1^{x}	3.9	79.4^{y}	6.1	74.8^{y}	4.8
1200	82.4^{x}	1.7	85.3^{x}	14.2	62.7^{z}	6.9	93.8	5.5	72.8^{y}	4.3
1500	76.3^{y}	3.7	57.9^{z}	1.4	84.7^{x}	11.7	56.8^{z}	7.4	104.4	10.4
1800	85.0^{x}	4.4	100.2	3.5	102.2	6.3	82.5^{x}	8.0	79.7^{y}	6.5
2400	142.5y	13.1	136.7^{x}	10.7	149.7^{z}	6.1	107.3	11.8	58.2^{z}	1.5
3000	111.7	7.0	98.7	3.4	109.2	13.0	75.9^{y}	7.0	83.4^{x}	8.0
3600	92.1	5.0	102.3	3.3	110.2	4.4	90.4	9.5	69.1^{z}	7.0

significance levels are: x<0.05; y<0.01; z<0.001

Figure
Click here to download high resolution image

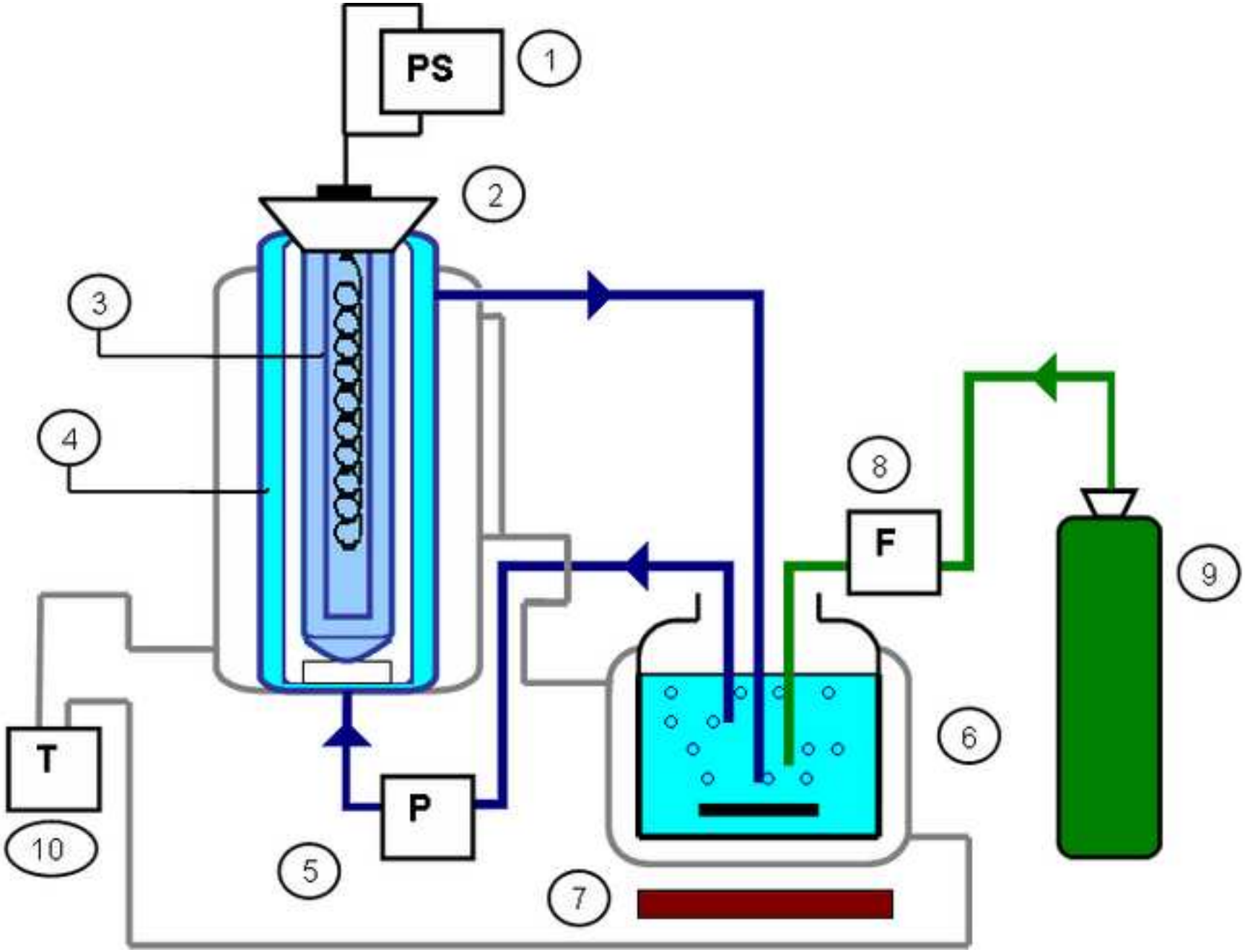

Figure

Click here to download high resolution image

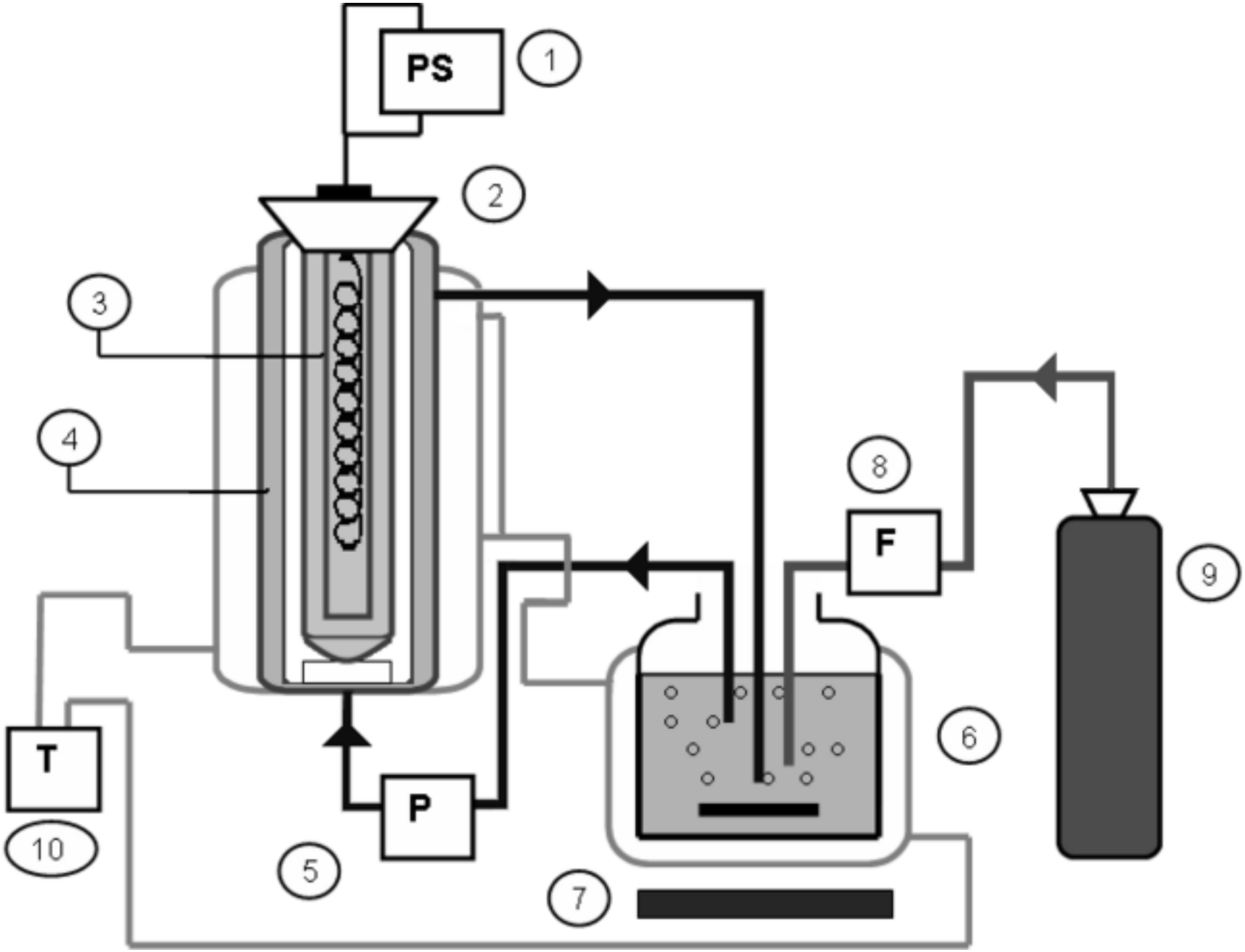

Figure

Click here to download Figure: Fig_2_pH.ppt

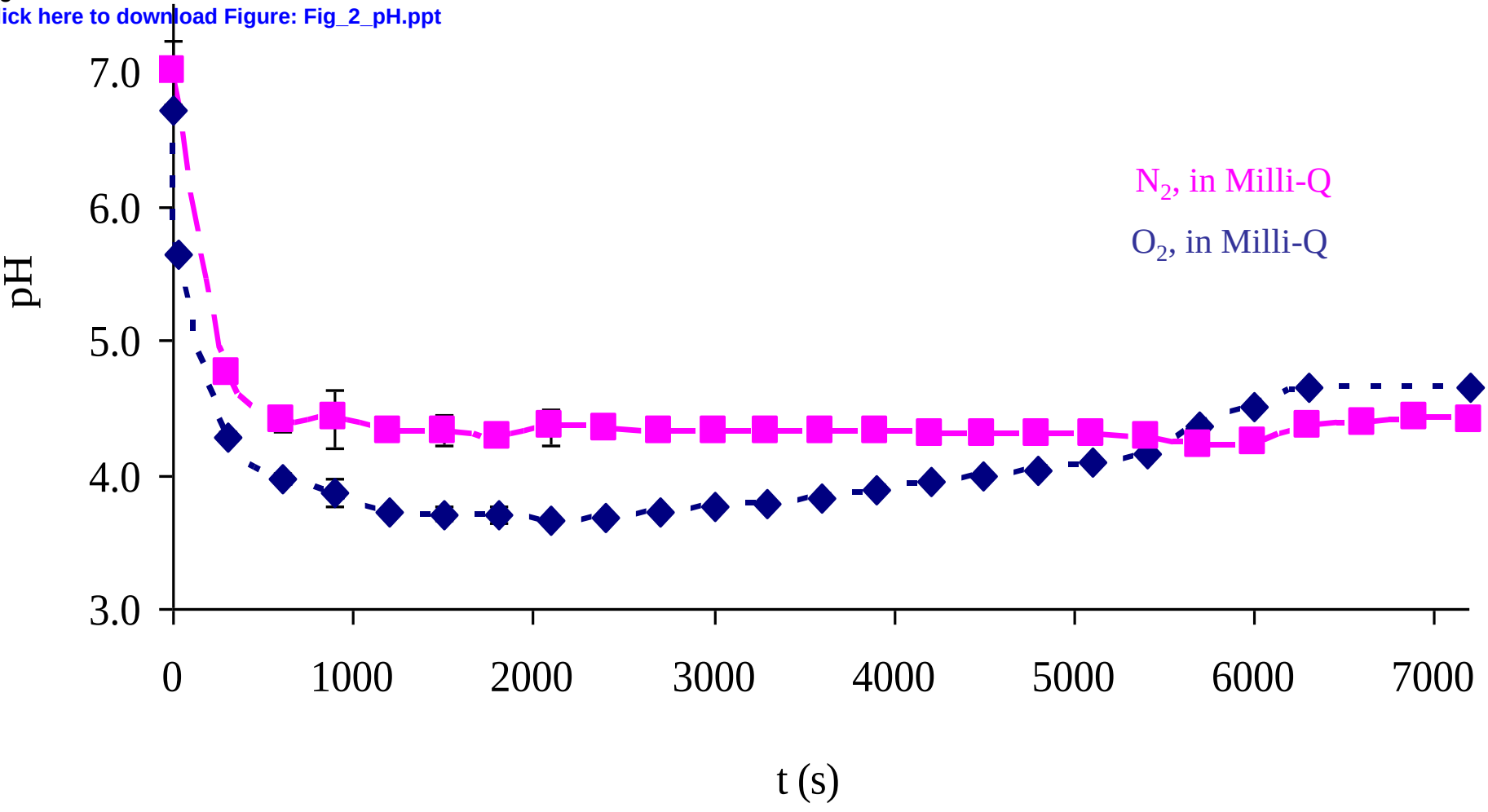

Figure

Click here to download Figure: Fig_2_bw_pH.ppt

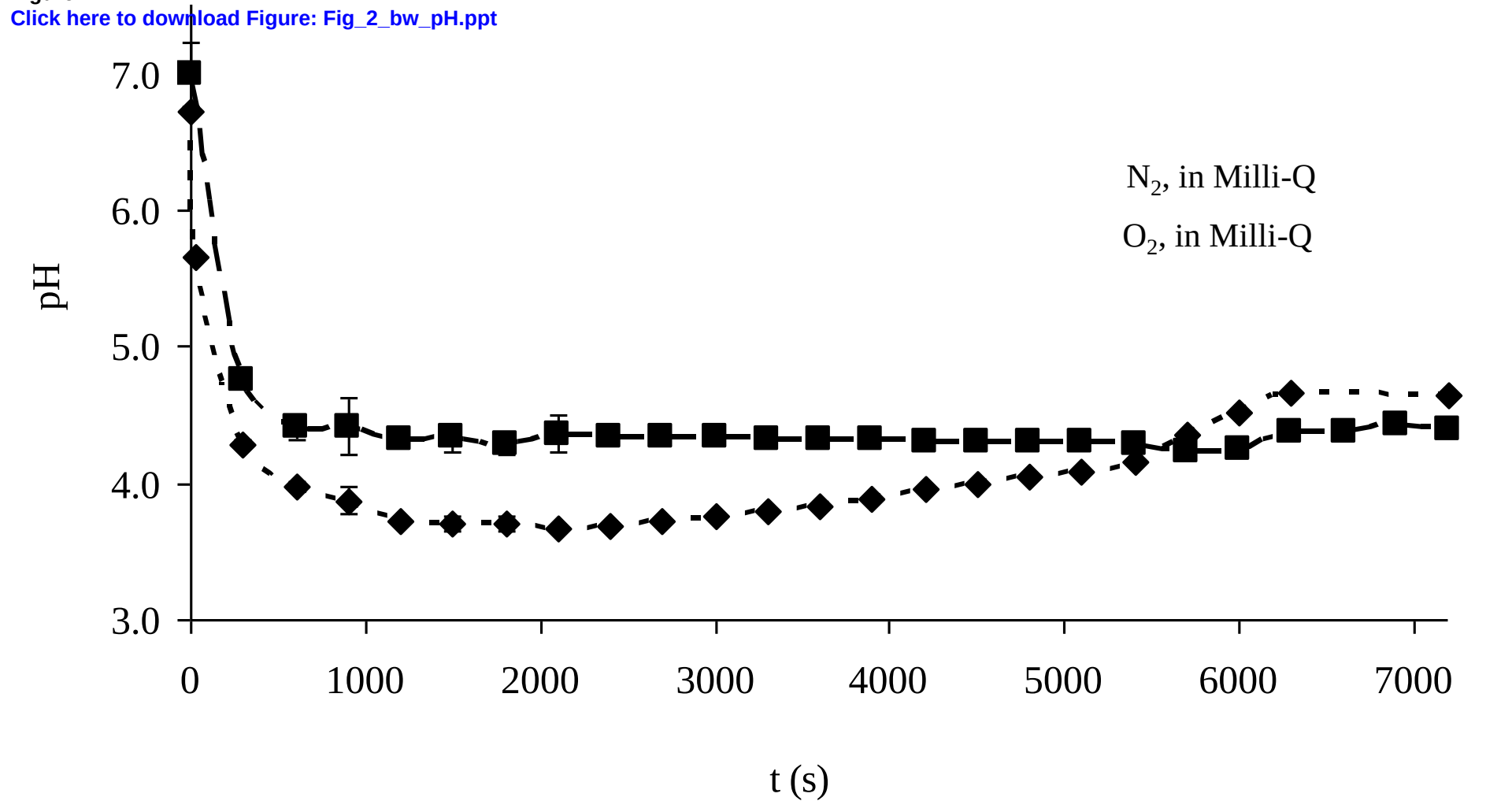

Figure

Click here to download Figure: Fig_3_buffer_effect_dicl.ppt

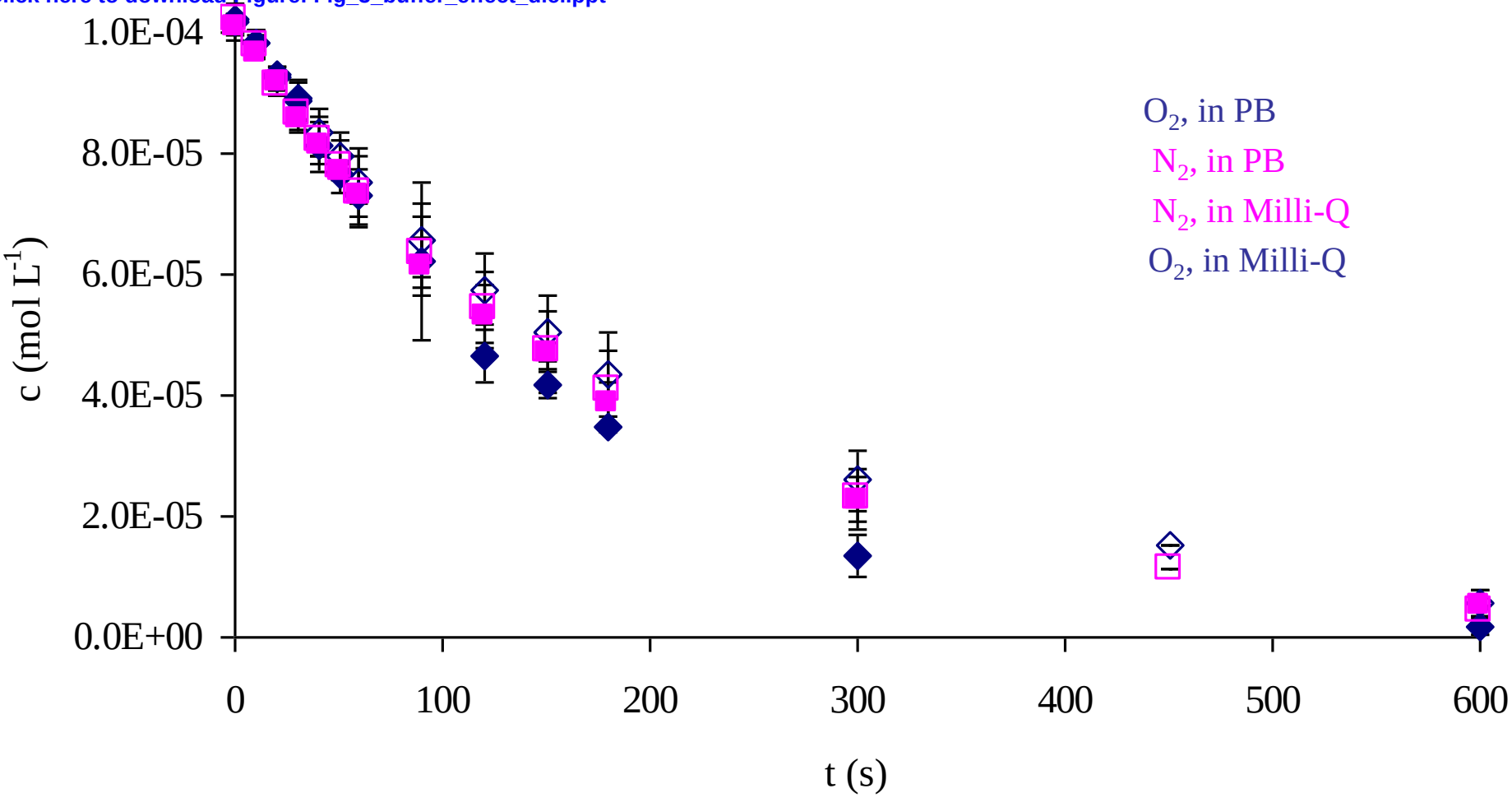

Figure

Click here to download Figure: Fig_3_bw_buffer_effect_dicl.ppt

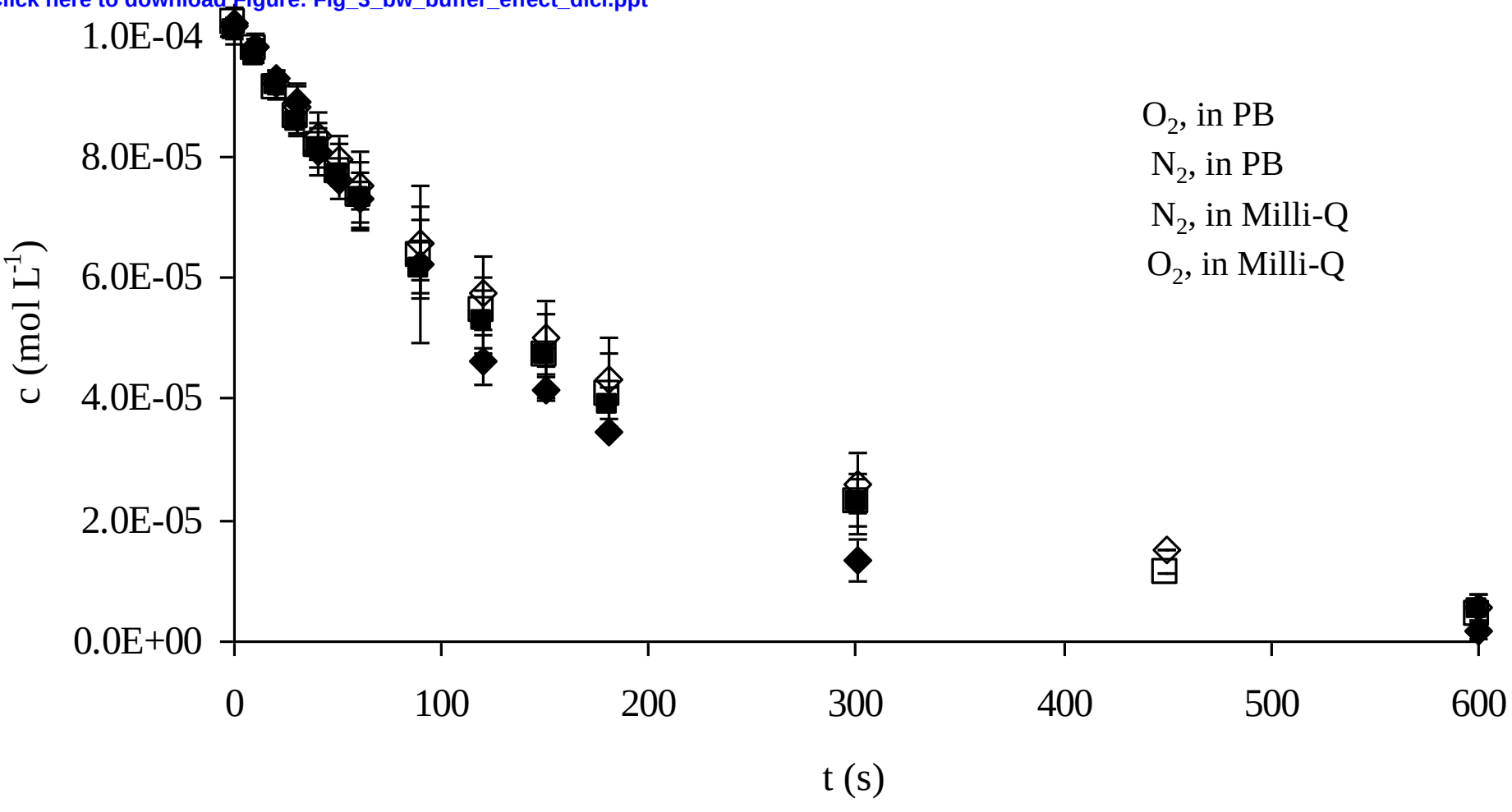

Figure
Click here to download Figure: Fig_4_buffer_effect_by_products.ppt

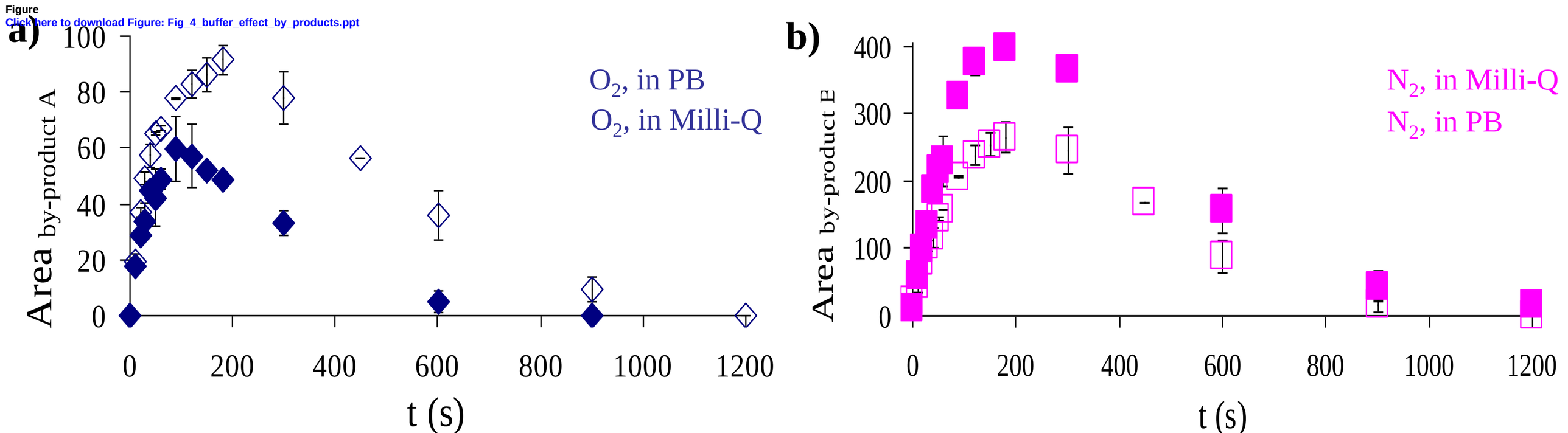

Figure

Click here to download Figure: Fig_4_bw_buffer_effect_by_products.ppt

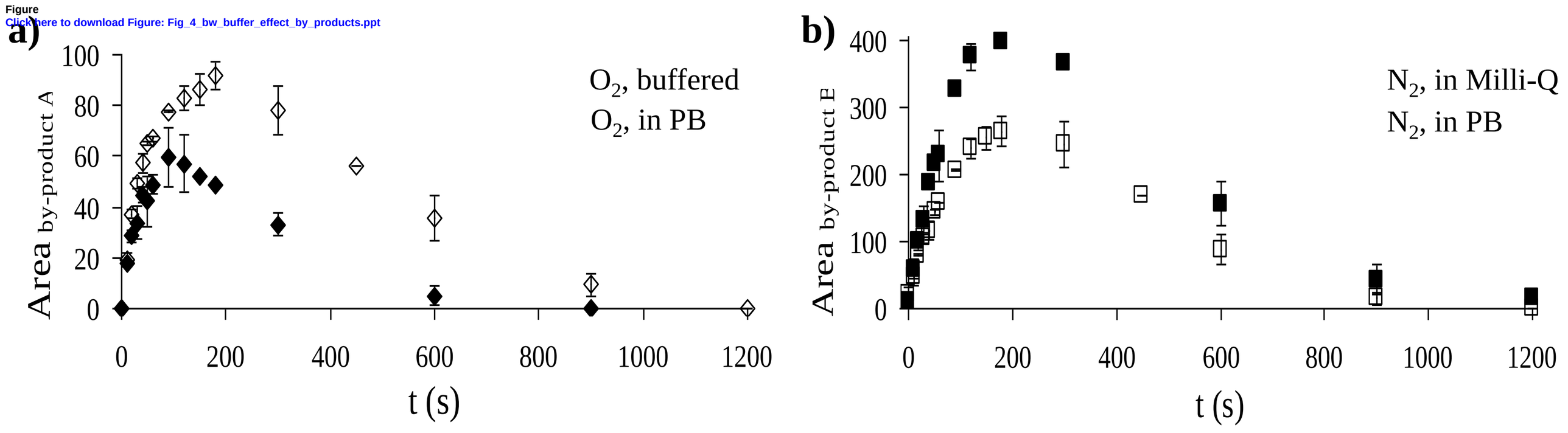

Figure

Click here to download Figure: Fig_5_buffer_effect_acids.ppt

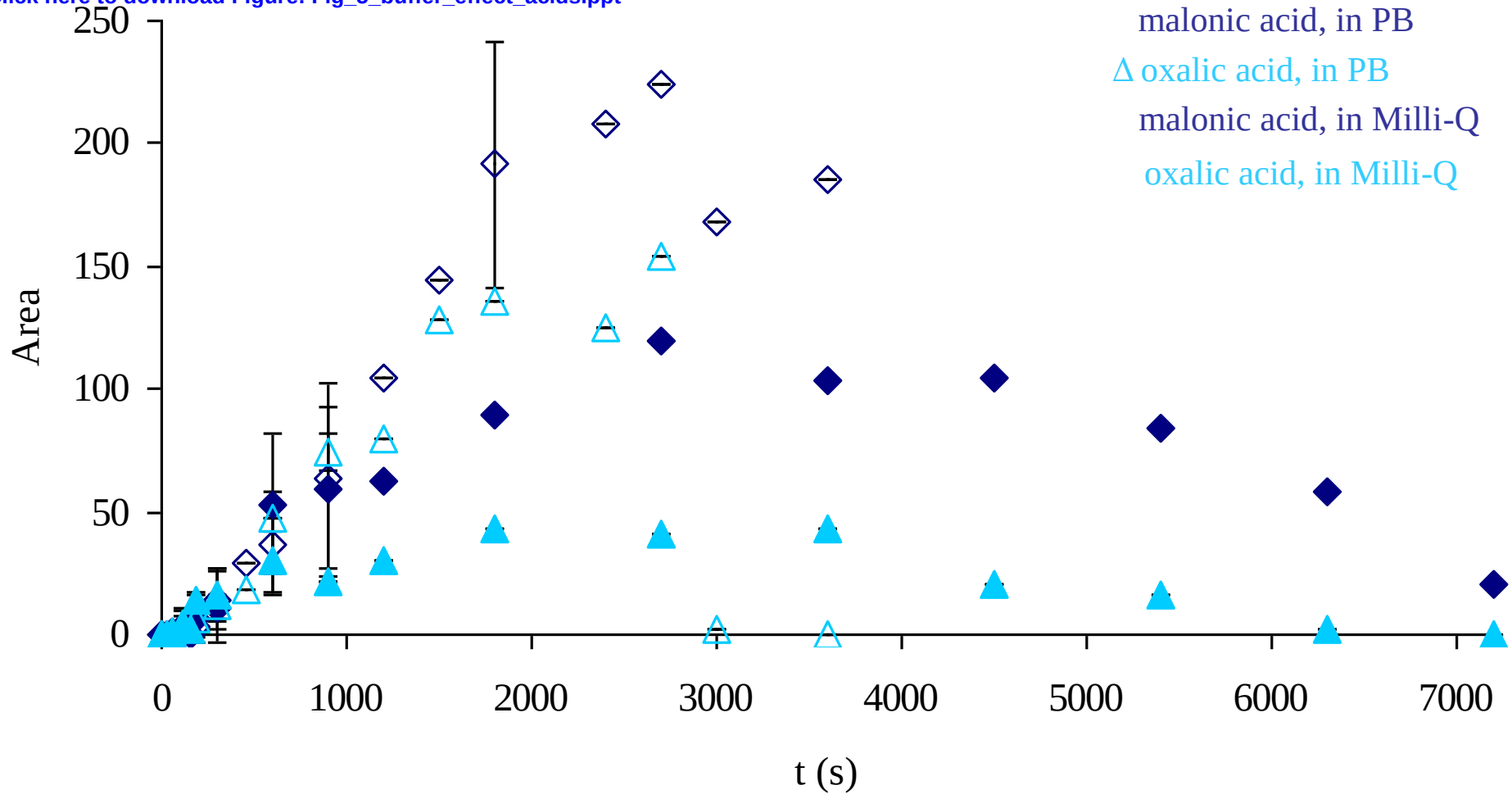

Figure

Click here to download Figure: Fig_5_bw_buffer_effect_acids.ppt

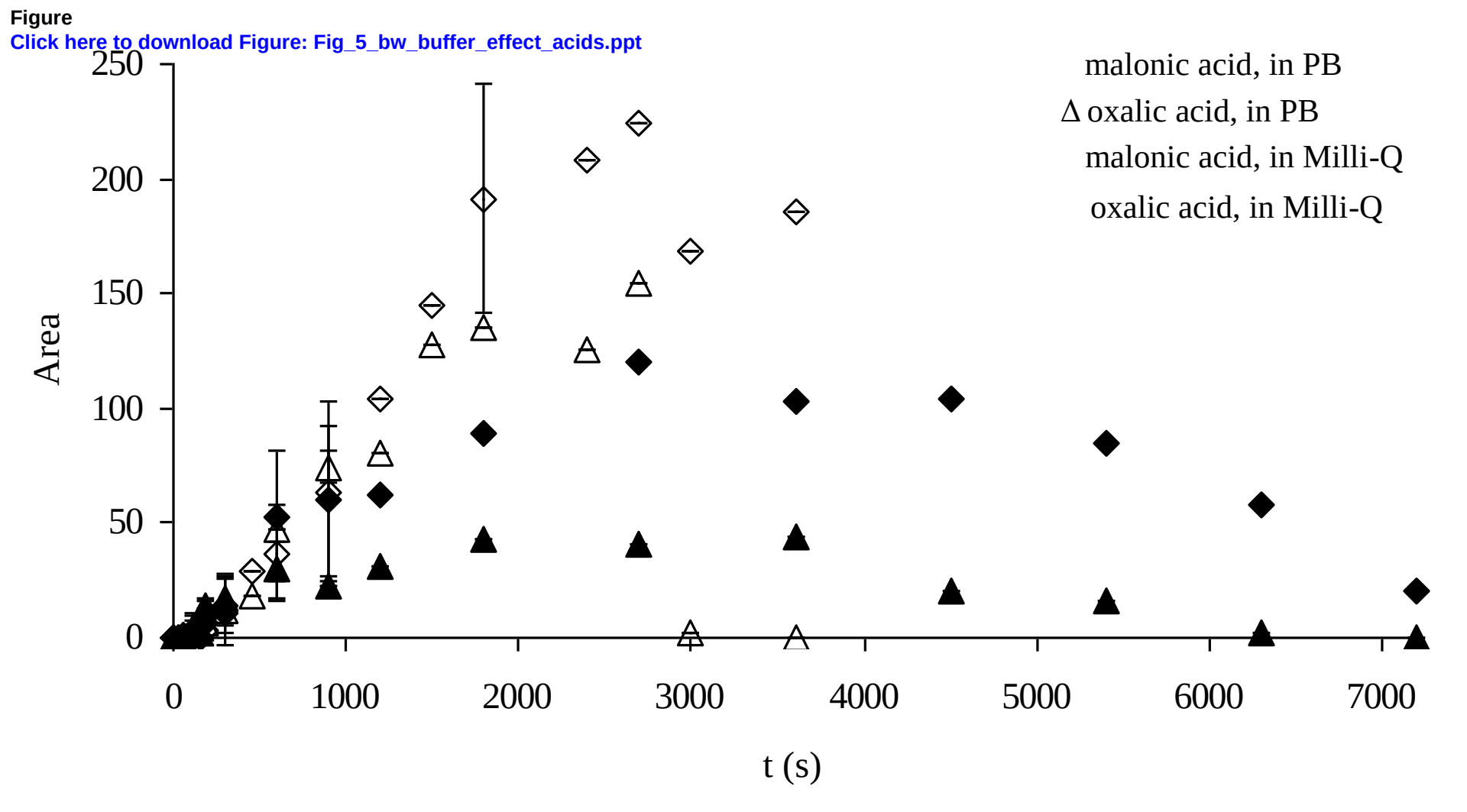

Figure
Click here to download Figure: Fig_6_O2_effect_by_products.ppt

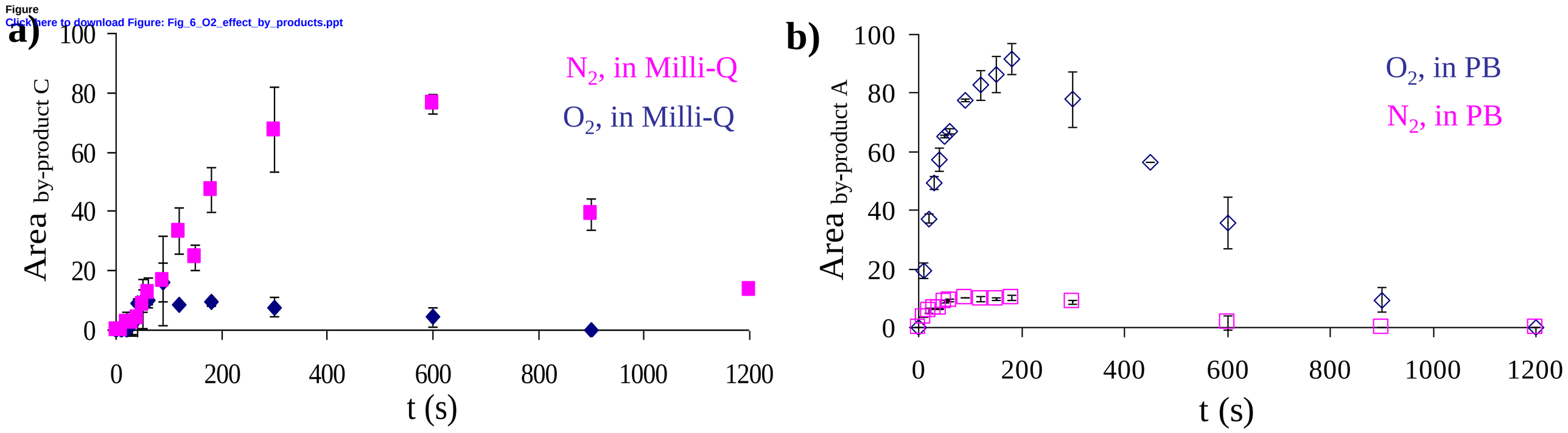

Figure
Click here to download Figure: Fig_6_bw_O2_effect_by_products.ppt

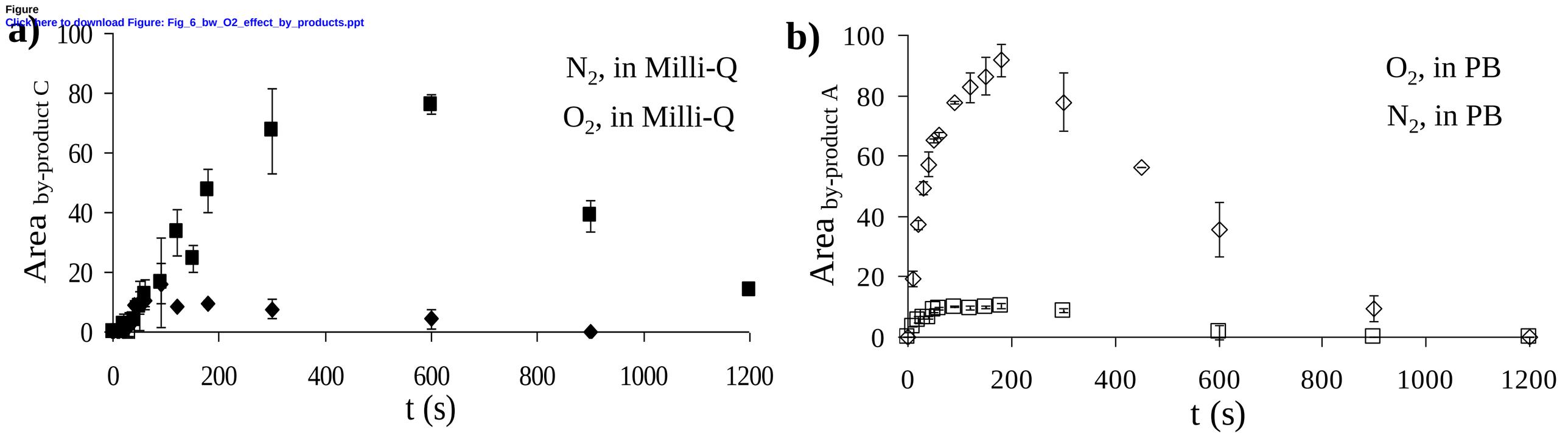

Figure

Click here to download Figure: Fig_7_AOX.ppt

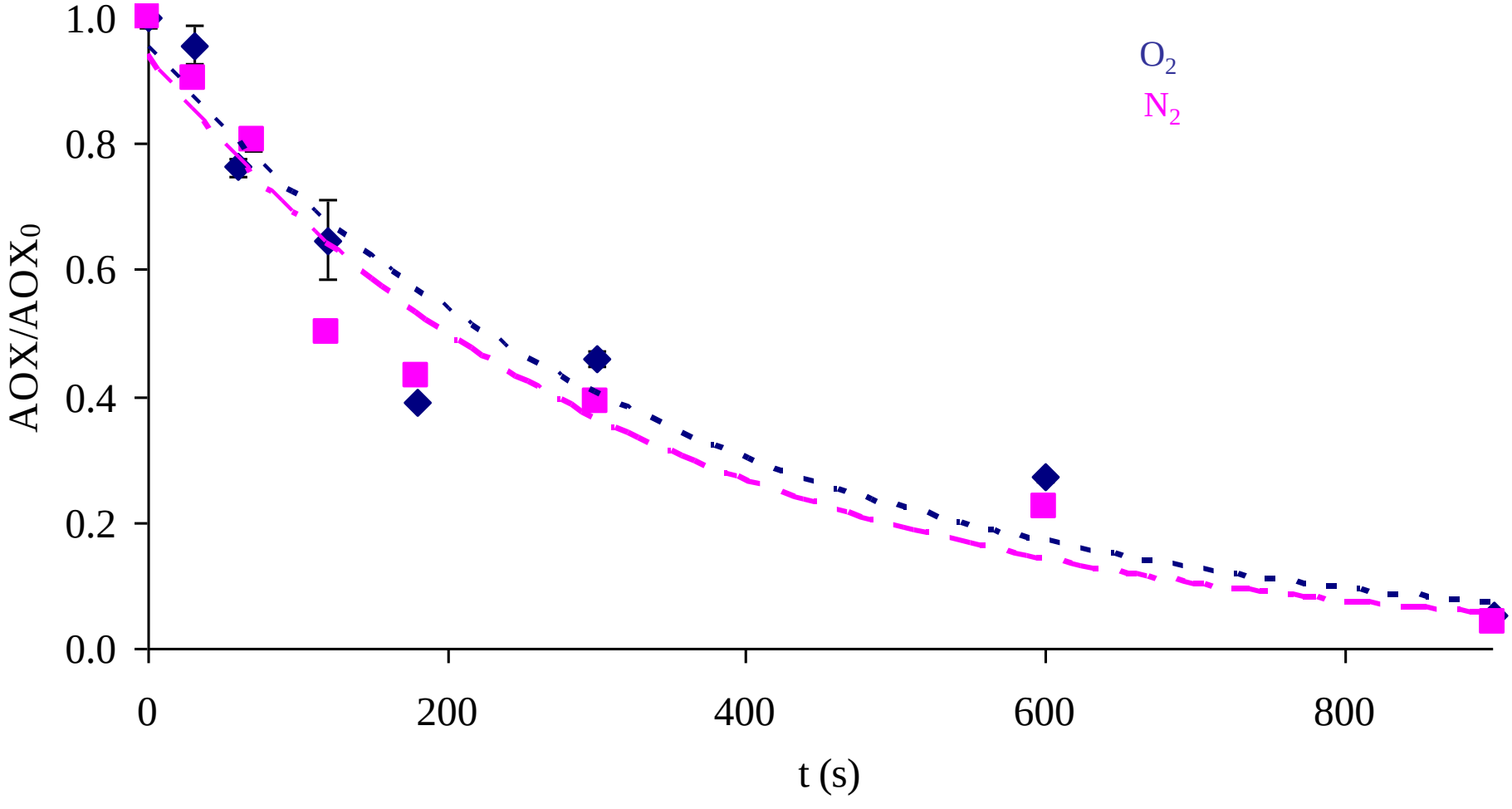

Figure

Click here to download Figure: Fig_7_bw_AOX.ppt

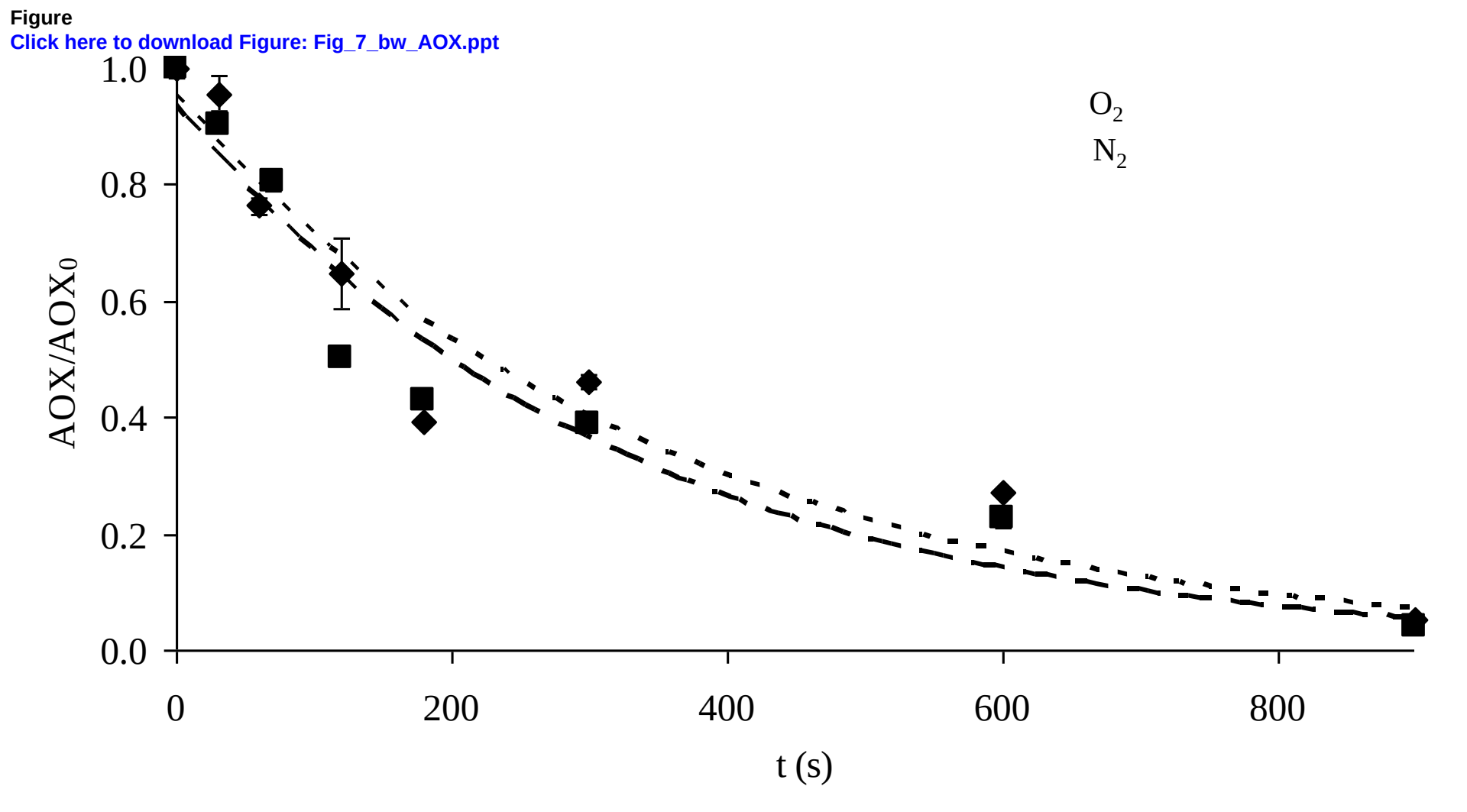

Figure

Click here to download Figure: Fig_8_toxicity_TOC.ppt

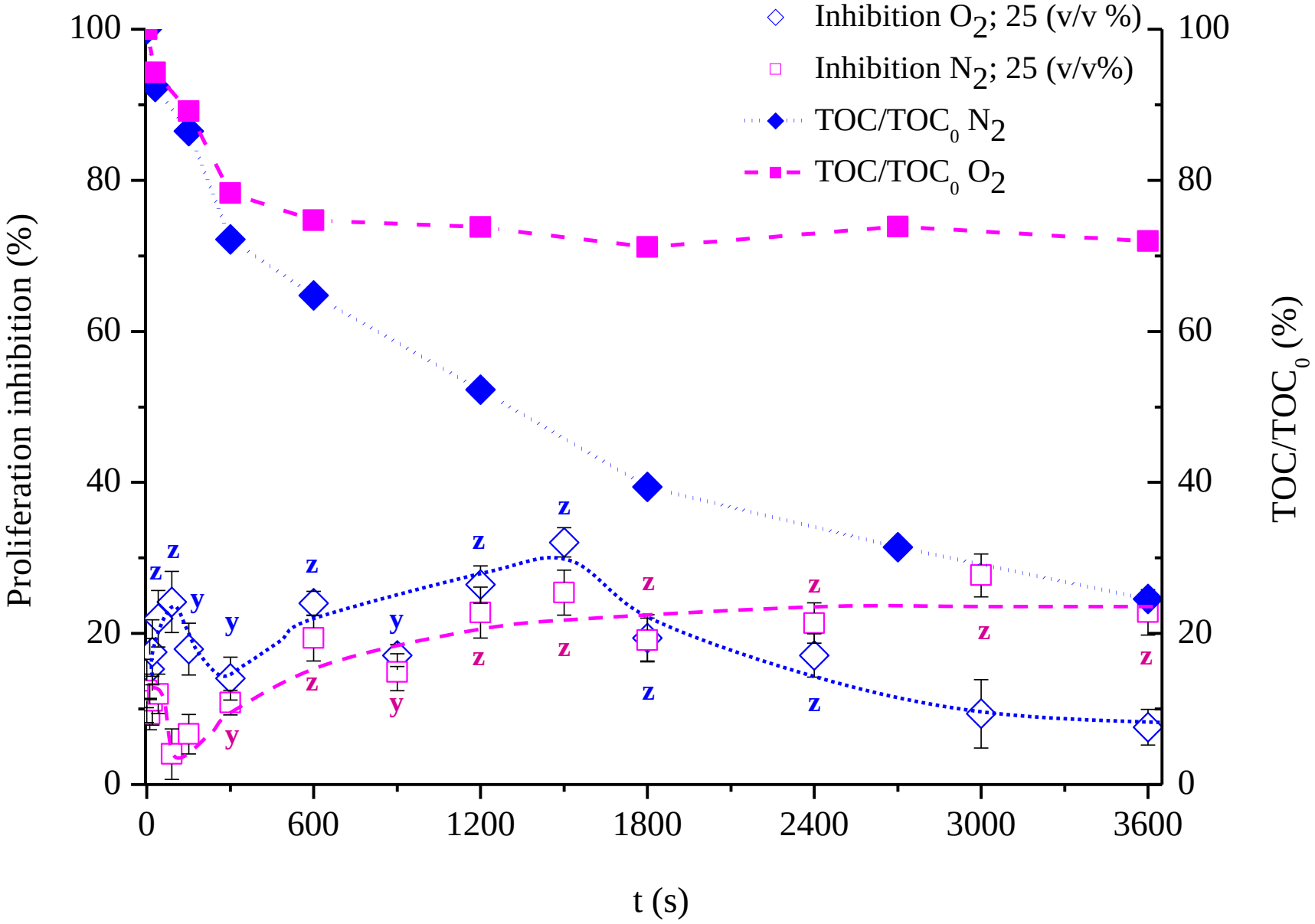

Figure

Click here to download Figure: Fig_8_bw_toxicity_TOC.ppt

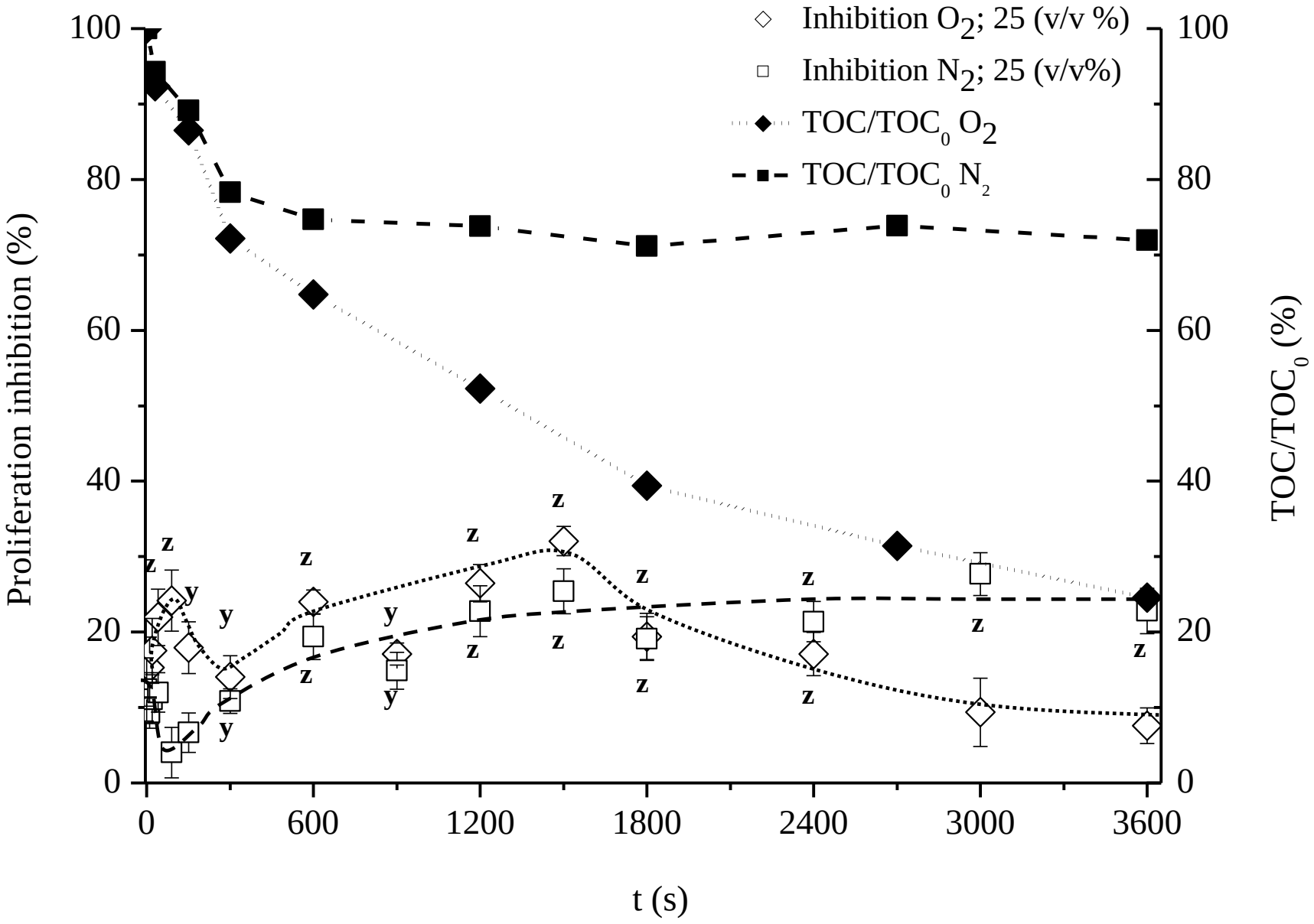

Figure

Click here to download Figure: Fig_9_effect_of_c0.ppt

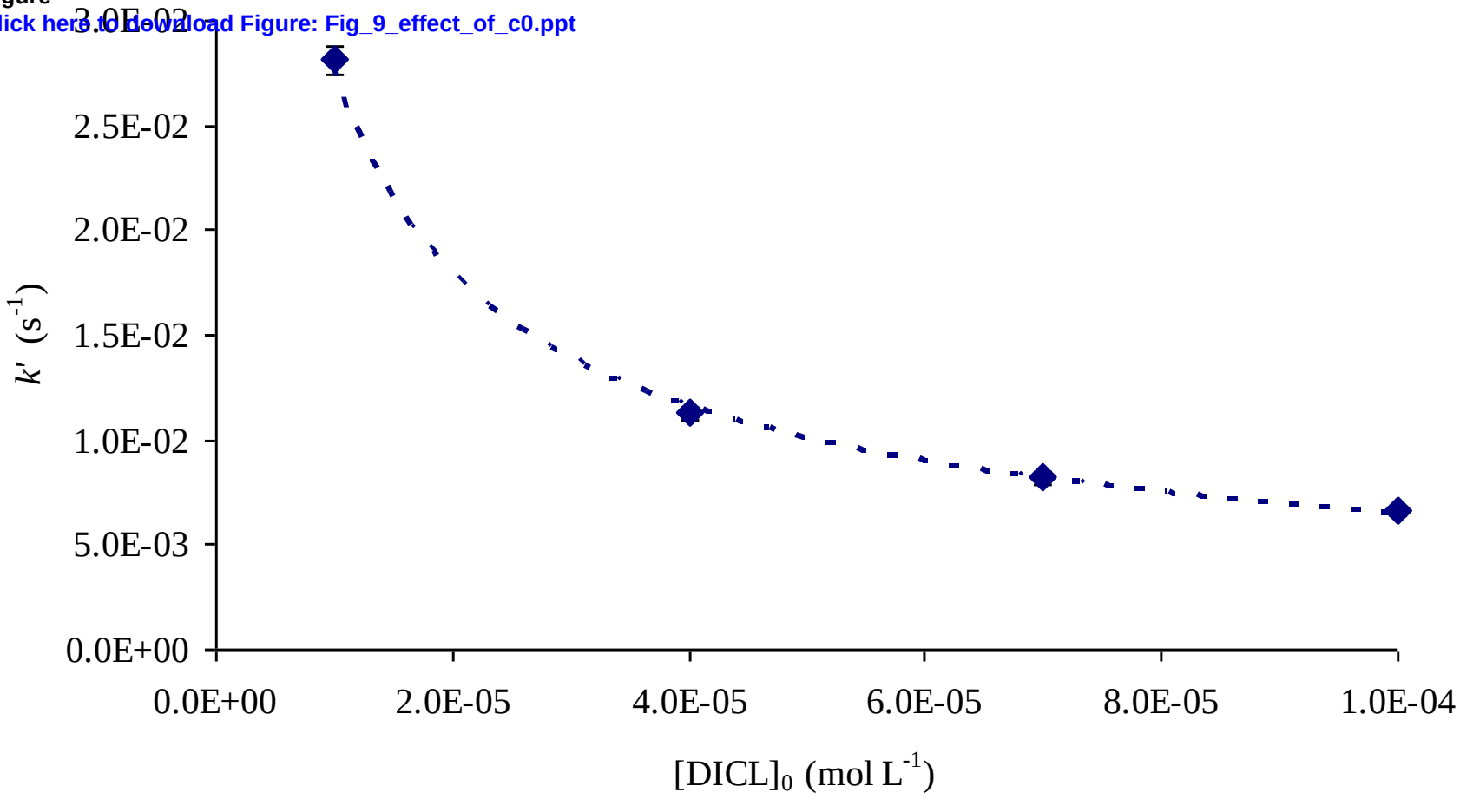

Figure

Click here to download Figure: Fig_9_bw_effect_of_c0.ppt

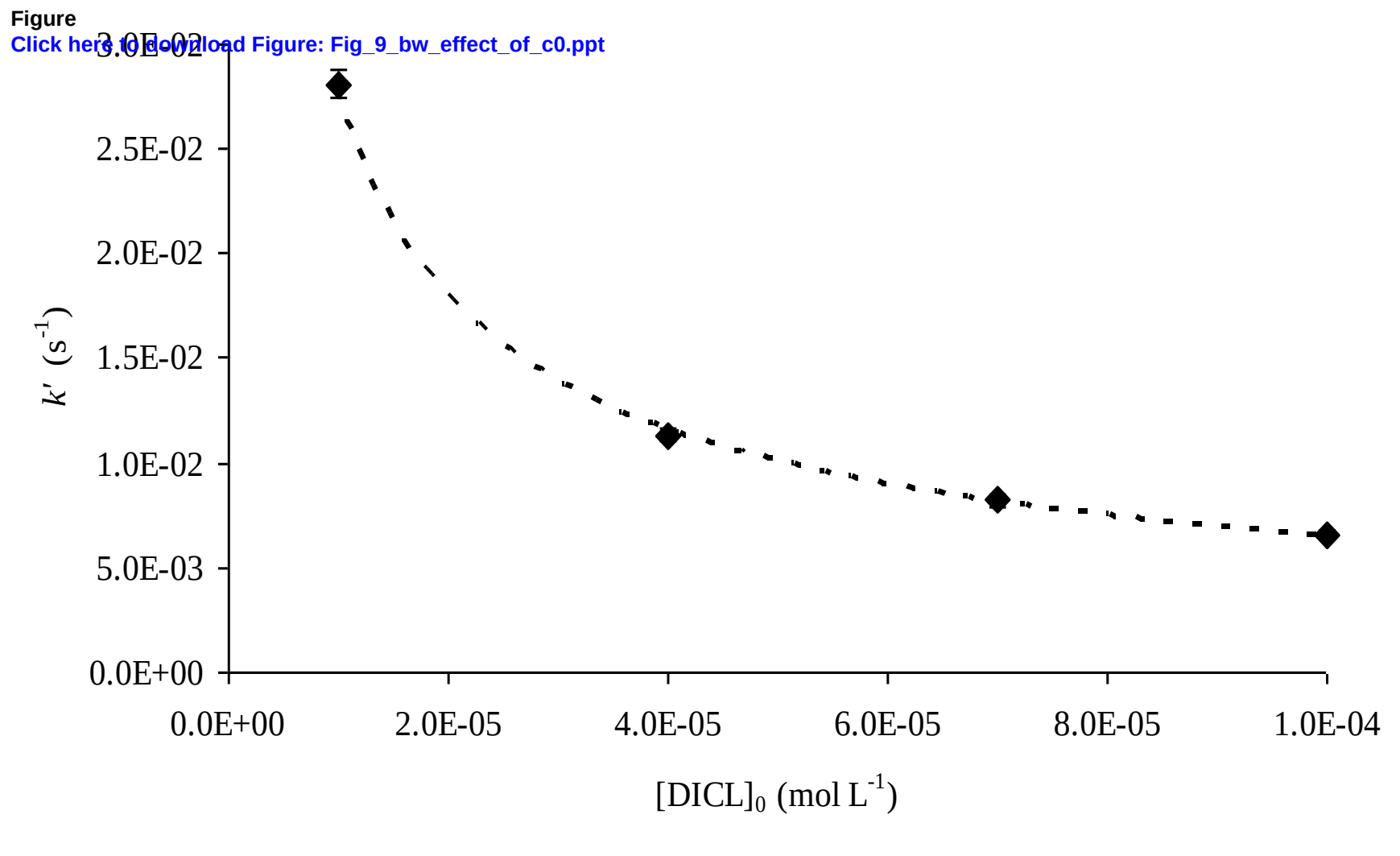

Figure

Click here to download Figure: Fig_10_UV_specta_by_products.ppt

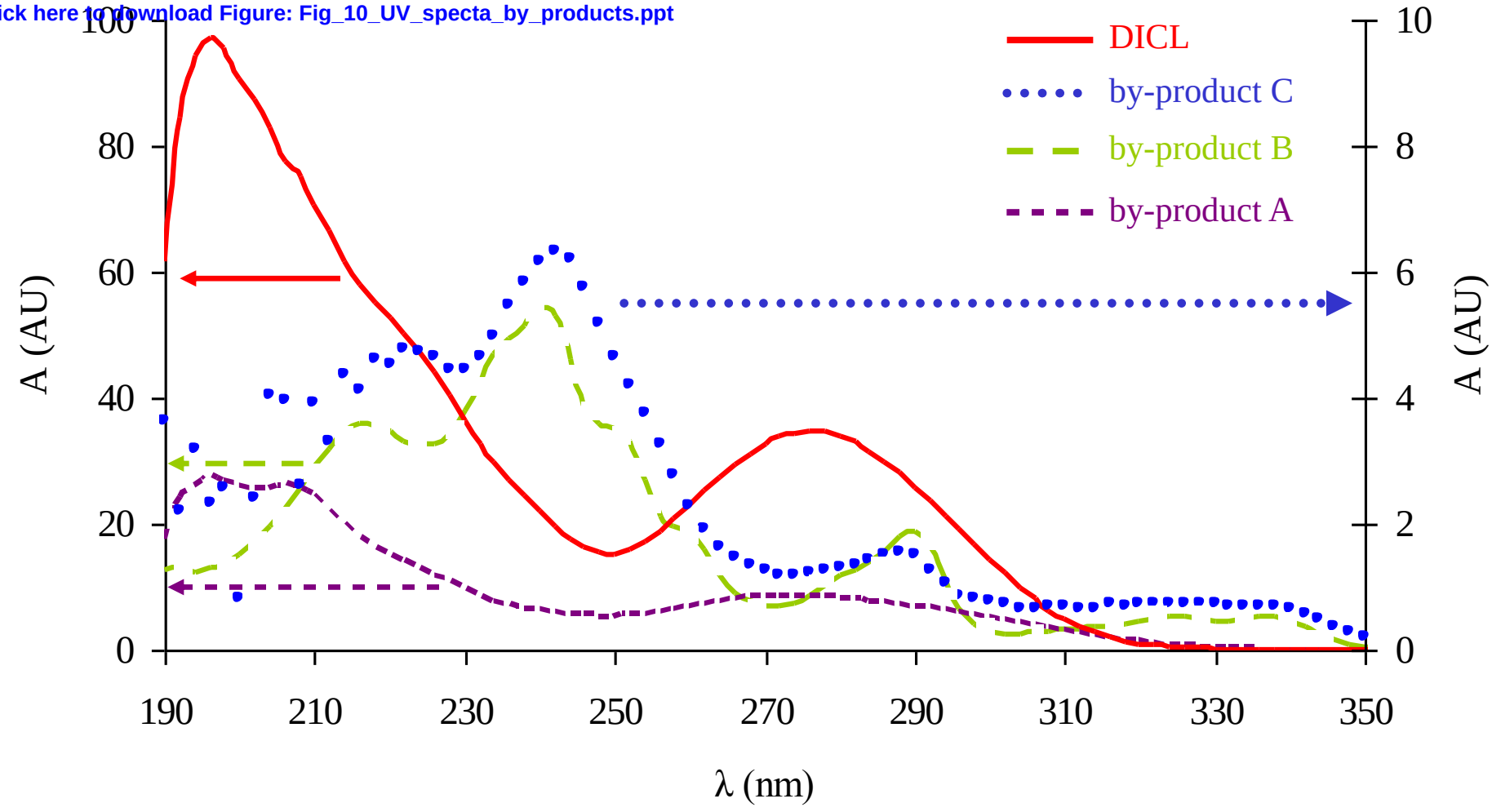

Figure

Click here to download Figure: Fig_10_bw_UV_specta_by_products2.ppt

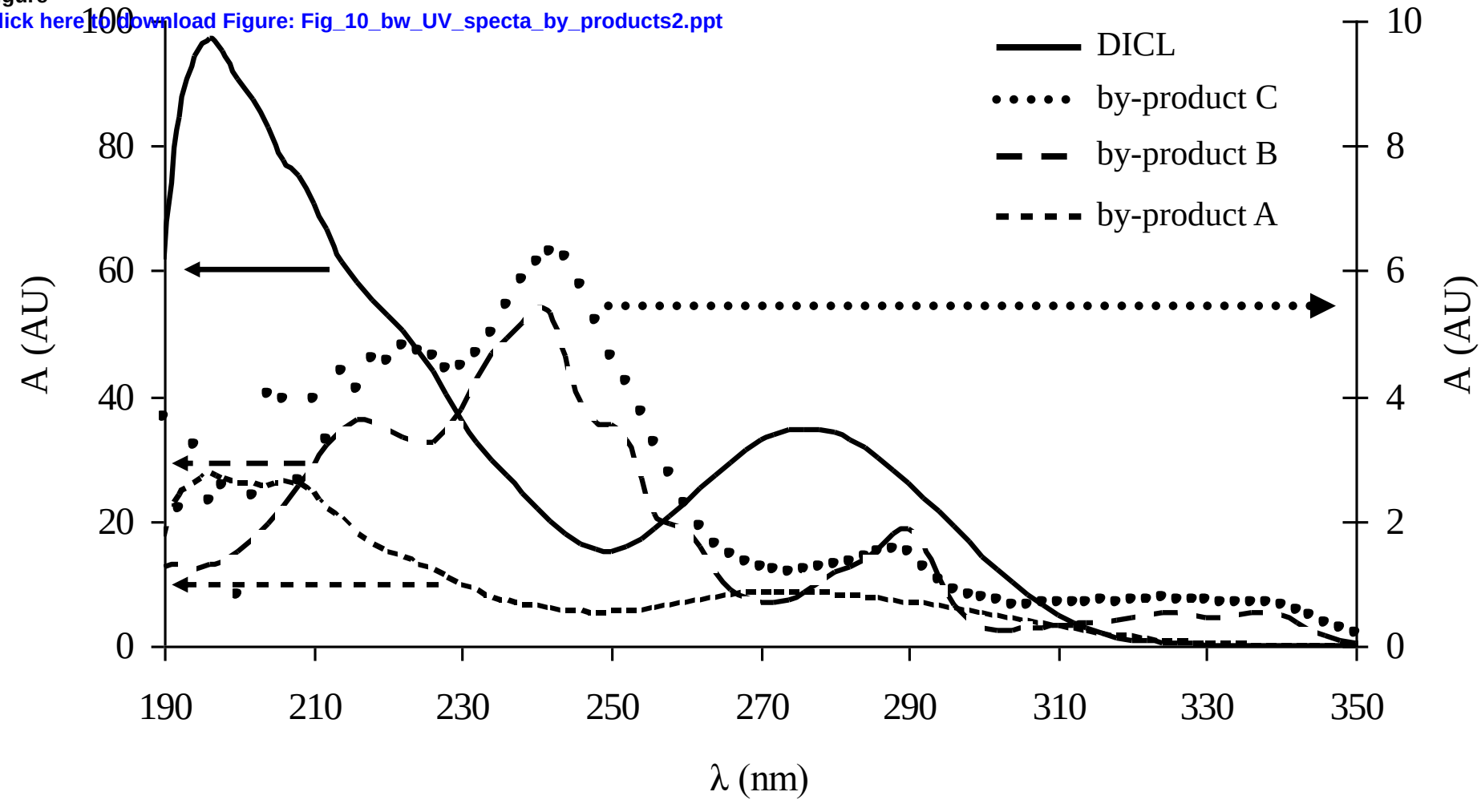

Figure

Click here to download Figure: Fig_11_by_products.ppt

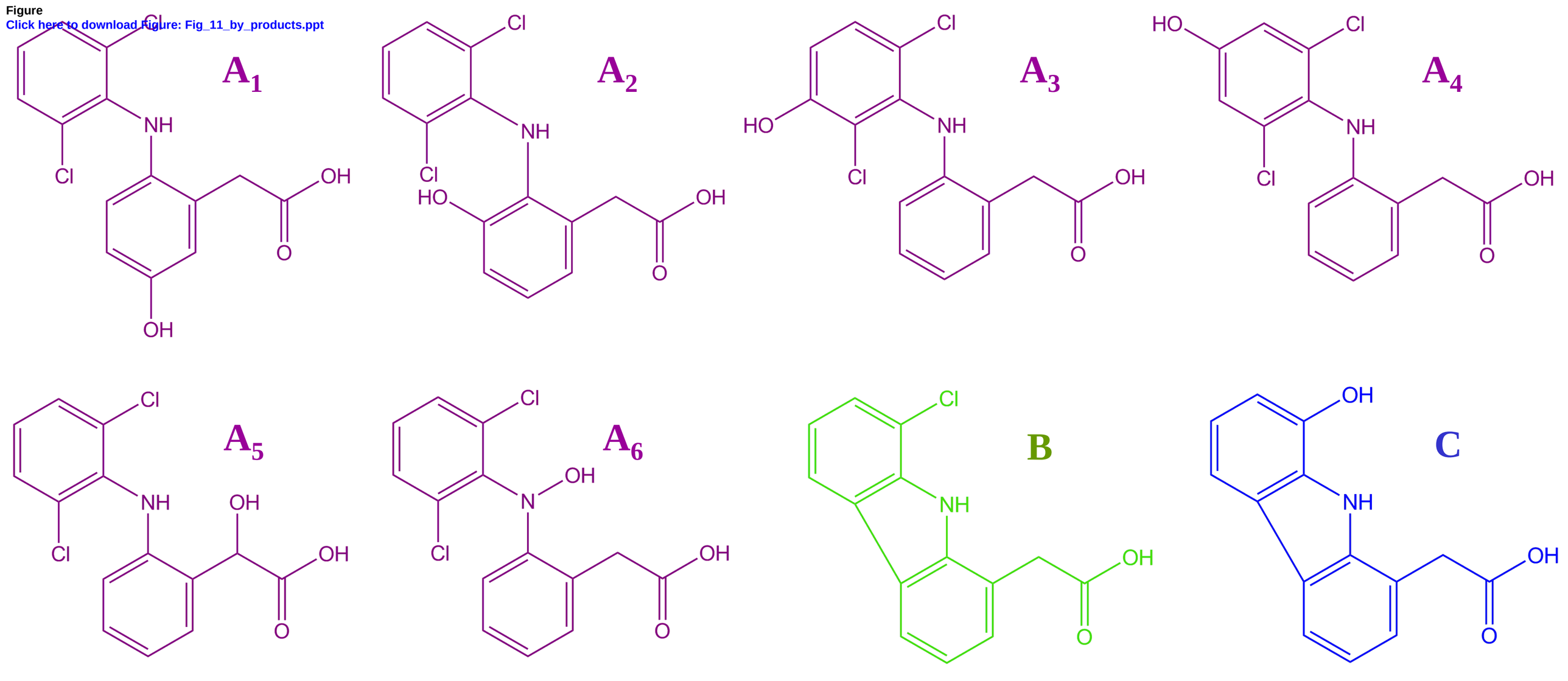

Figure

Click here to download Figure: Fig_11_bw_by_products.ppt

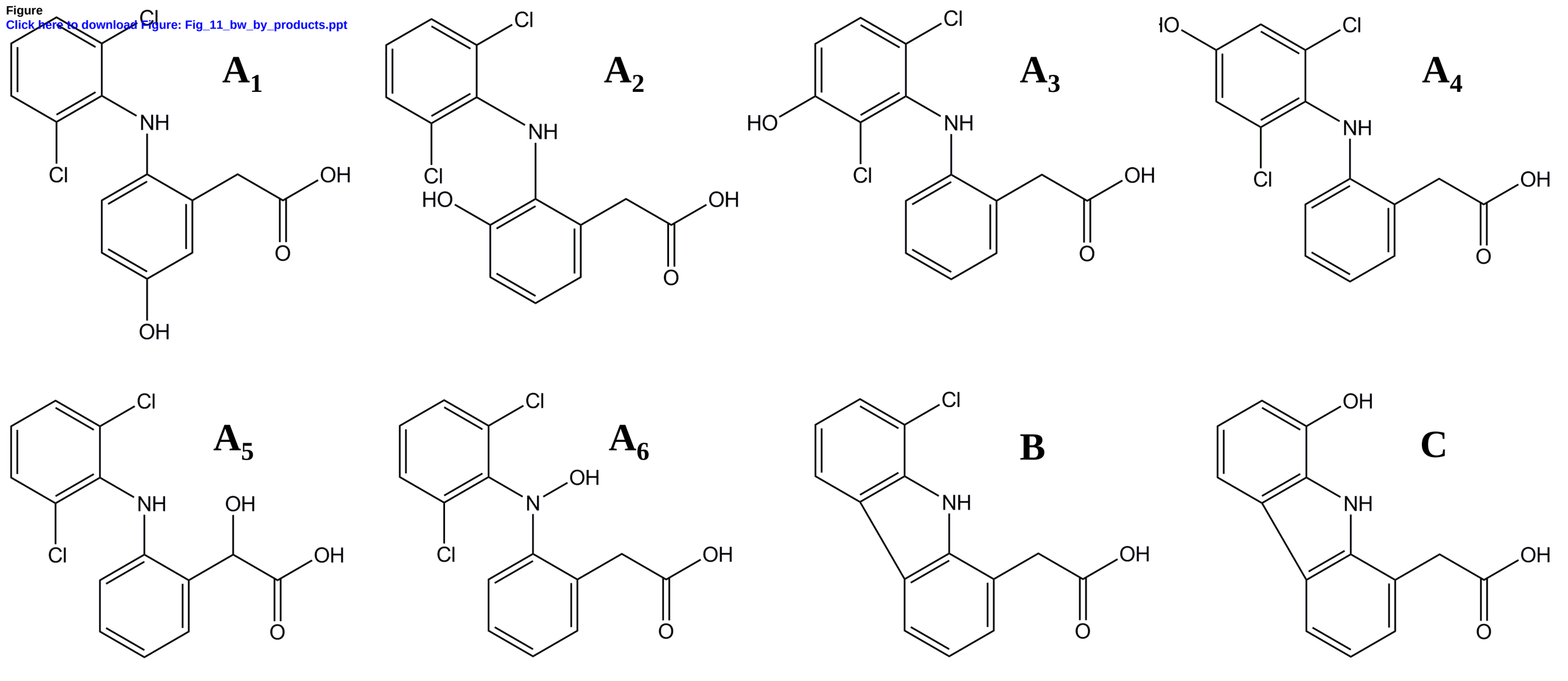

Figure

Click here to download Figure: Fig_12_chemotaxis.ppt

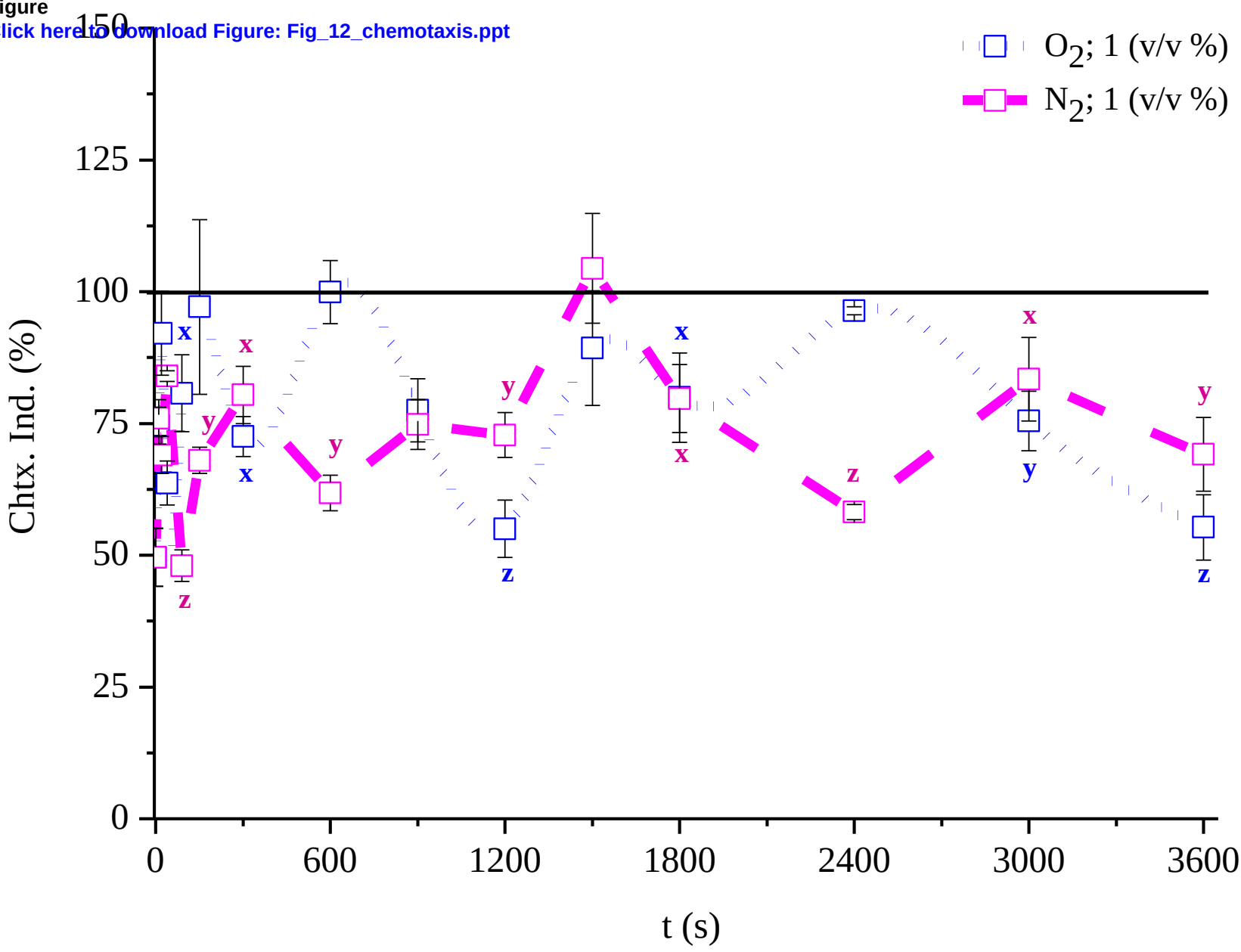

Figure

Click here to download Figure: Fig_12_bw_chemotaxis.ppt

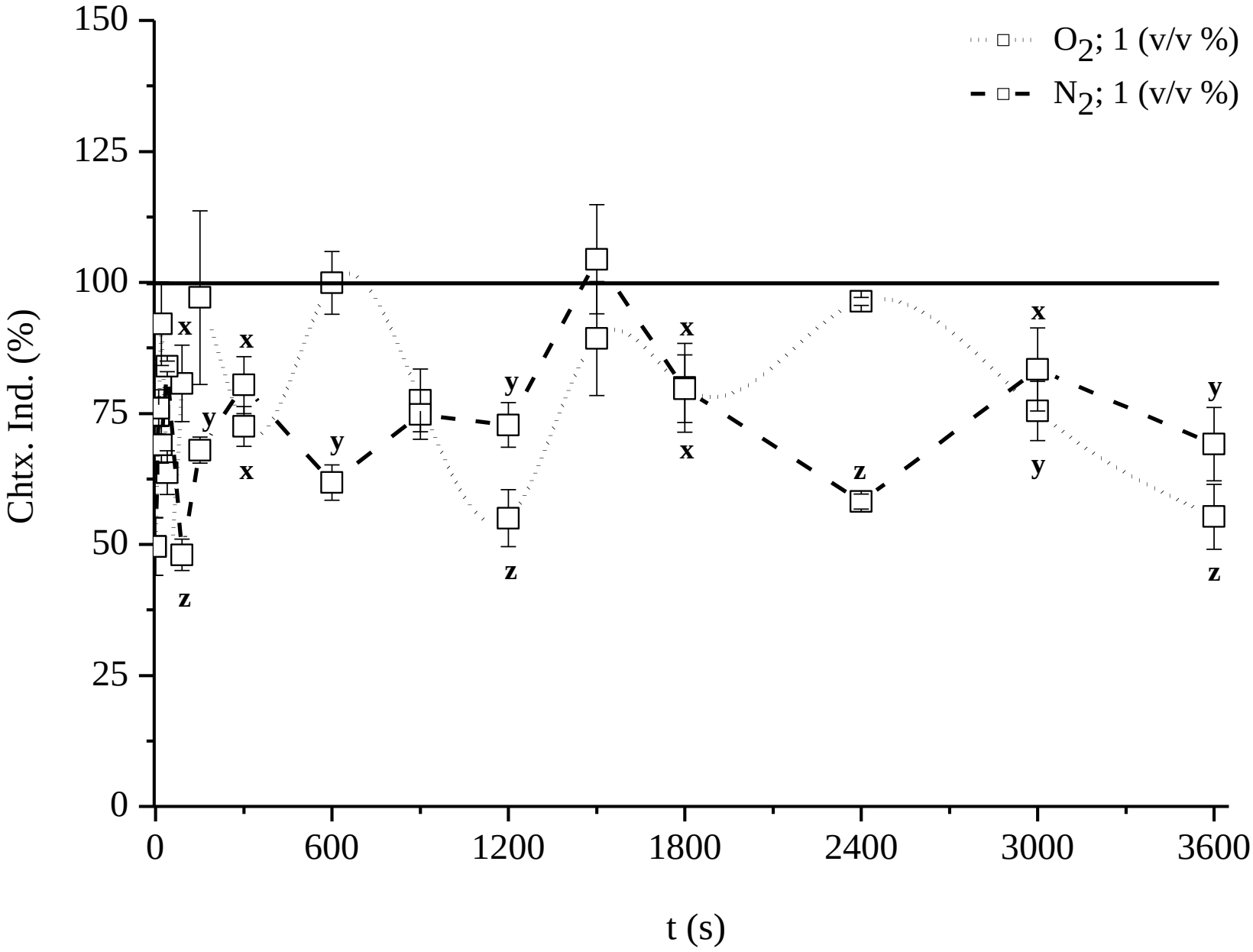

Figure

Click here to download Figure: Fig_13_sheme.ppt

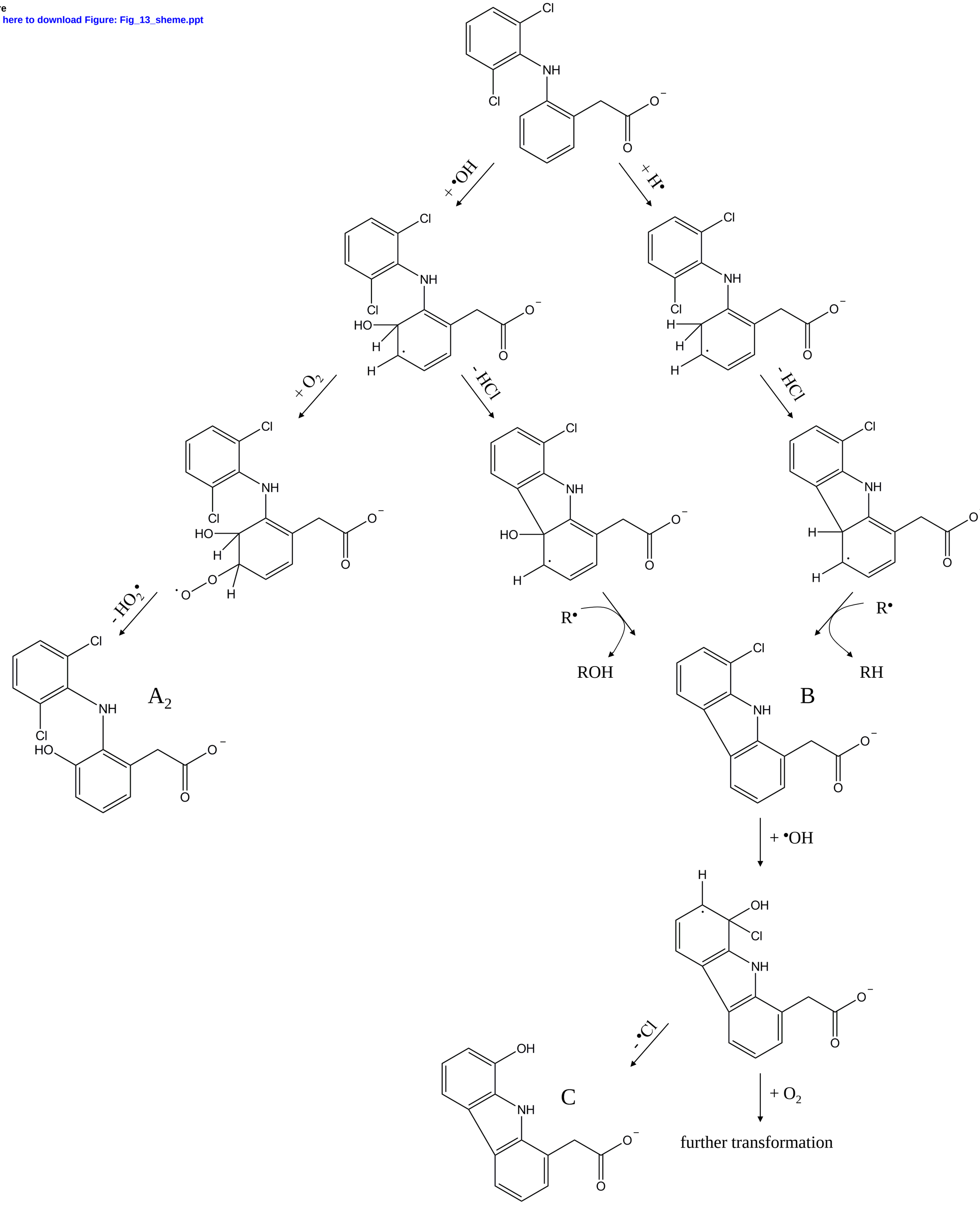

Supplementary Material

Click here to download Supplementary Material: SupplementaryMaterial.doc

Conflict of interest

Hereby, all authors of the manuscript entitled "Vacuum ultraviolet photolysis of diclofenac and the effect of the treated aqueous solutions on the proliferation and migratory responses of *Tetrahymena pyriformis*" disclose any actual or potential conflict of interest including any financial, personal or other relationships with other people or organizations within three years of beginning the submitted work that could inappropriately influence, or be perceived to influence, their work.

2013.05.09.

Eszter Arany

Júlia Láng

Dávid Somogyvári

Orsolya Láng

Tünde Alapi

István Ilisz

Krisztina Gajda-Schrantz

András Dombi

László Kőhidai

Klára Hernádi